

A PARAMETER ERROR IDENTIFICATION METHOD FOR POWER PLANT
DYNAMIC MODELS

A THESIS SUBMITTED TO
THE GRADUATE SCHOOL OF NATURAL AND APPLIED SCIENCES
OF
MIDDLE EAST TECHNICAL UNIVERSITY

BY

ETKI AÇILAN

IN PARTIAL FULFILLMENT OF THE REQUIREMENTS
FOR
THE DEGREE OF MASTER OF SCIENCE
IN
ELECTRICAL AND ELECTRONICS ENGINEERING

JUNE 2022

Approval of the thesis:

**A PARAMETER ERROR IDENTIFICATION METHOD FOR POWER
PLANT DYNAMIC MODELS**

submitted by **ETKI AÇILAN** in partial fulfillment of the requirements for the degree
of **Master of Science in Electrical and Electronics Engineering Department,**
Middle East Technical University by,

Prof. Dr. Halil Kalıpçılar
Dean, Graduate School of **Natural and Applied Sciences** _____

Prof. Dr. İlkay Ulusoy
Head of Department, **Electrical and Electronics Engineering** _____

Assoc. Prof. Dr. Murat Göl
Supervisor, **Electrical and Electronics Engineering, METU** _____

Examining Committee Members:

Prof. Dr. Ali Nezih Güven
Electrical and Electronics Engineering Dept., METU _____

Assoc. Prof. Dr. Murat Göl
Electrical and Electronics Engineering Dept., METU _____

Assoc. Prof. Dr. Ozan Keysan
Electrical and Electronics Engineering Dept., METU _____

Prof. Dr. Saffet Ayasun
Electrical and Electronics Engineering Dept., Gazi University _____

Assist. Prof. Dr. Oğuzhan Ceylan
Electrical and Electronics Engineering Dept., Marmara University _____

Date: 30.06.2022

I hereby declare that all information in this document has been obtained and presented in accordance with academic rules and ethical conduct. I also declare that, as required by these rules and conduct, I have fully cited and referenced all material and results that are not original to this work.

Name, Surname: Etki Açılan

Signature :

ABSTRACT

A PARAMETER ERROR IDENTIFICATION METHOD FOR POWER PLANT DYNAMIC MODELS

Açılan, Etki

M.S., Department of Electrical and Electronics Engineering

Supervisor: Assoc. Prof. Dr. Murat Göl

June 2022, 52 pages

Incorrect parameters in a power plant dynamic model affect the analysis results and control decisions in a power system, which may have serious consequences. The on-line calibration techniques in the literature utilize sensitivity analysis to determine the identifiable parameters before the calibration, and treat majority of sensitive parameters as potentially erroneous. Hence, the candidate parameter subset for calibration mostly consists of distractors, i.e. highly sensitive but already correct parameters. The inclusion of distractors in the parameter calibration may decrease the accuracy of calibration, and increase the computation time. This thesis proposes a method to identify erroneous parameters through the mismatch between collected PMU measurements and power plant model response. The proposed method relies on the classification of Recurrence Plots of the mismatch using 2-D Convolutional Neural Networks, and identifies the erroneous parameters via the orthogonal decomposition. Hence, a smaller subset of candidate parameters is obtained by eliminating the distractors.

Keywords: Power Plant Parameter Calibration, Convolutional Neural Networks, Dy-

dynamic Parameter Estimation, Collinearity, Identifiability, Time Series Classification

ÖZ

GÜÇ SANTRALLERİNİN DİNAMİK MODELLERİNDE HATALI PARAMETRE BELİRLEME METODU

Açılan, Etki

Yüksek Lisans, Elektrik ve Elektronik Mühendisliği Bölümü

Tez Yöneticisi: Doç. Dr. Murat Göl

Haziran 2022 , 52 sayfa

Bir enerji santrali dinamik modelindeki yanlış parametreler, bir güç sistemindeki analiz sonuçlarını ve kontrol kararlarını etkiler ve bu da ciddi sonuçlara yol açabilir. Literatürdeki çevrimiçi kalibrasyon teknikleri, kalibrasyondan önce tanımlanabilir parametreleri belirlemek için duyarlılık analizini kullanır ve hassas parametrelerin çoğunu potansiyel olarak hatalı olarak ele alır. Bu nedenle, kalibrasyon için aday parametre alt kümesi çoğunlukla çeldiricilerden, yani oldukça hassas ancak zaten doğru parametrelerden oluşur. Parametre kalibrasyonuna çeldiricilerin dahil edilmesi, kalibrasyonun doğruluğunu azaltabilir ve hesaplama süresini artırabilir. Bu tez, toplanan PMU ölçümleri ve enerji santrali model reaksiyonu arasındaki uyumsuzluk yoluyla hatalı parametreleri belirlemek için bir yöntem önermektedir. Önerilen yöntem, 2-D Evrişimli Sinir Ağları kullanılarak uyumsuzluğun Tekrarlama Grafiklerinin sınıflandırılmasına dayanır ve ortogonal ayrıştırma yoluyla hatalı parametreleri tanımlar. Bu sayede, çeldiriciler ortadan kaldırılarak daha küçük bir aday parametre alt kümesi elde edilir.

Anahtar Kelimeler: Güç Santrallerinde Parametre Kalibrasyonu, Evrişimli sinir ağları, Dinamik Parametre Kestirimi, Doğrudaşlık, Belirlenebilirlik, Zaman Serileri Sınıflandırma

To Ramis Açılan.

ACKNOWLEDGMENTS

First, I would like to thank Dr. Murat Gol, my advisor, for guiding me through my master's degree. I was very lucky to have such an advisor during the last three years.

I also thank Scientific and Technological Research Council of Turkey (TUBITAK) for financially supporting me through my master's education via BİDED 2210-A Graduate Student Scholarship.

I also thank to my family and my friends in E-101, who supported me. Specifically, I want to thank Tuna Yildiz for sharing all of his knowledge and experience as well as his friendship with me.

Lastly, I want to thank my biggest motivation source, Sedef Eski, for her love, friendship, patience. I would not come this far without her.

TABLE OF CONTENTS

ABSTRACT	v
ÖZ	vii
ACKNOWLEDGMENTS	x
TABLE OF CONTENTS	xi
LIST OF TABLES	xiii
LIST OF FIGURES	xiv
LIST OF ABBREVIATIONS	xvi
CHAPTERS	
1 INTRODUCTION	1
1.1 The Contribution of the Thesis	3
1.2 The Outline of the Thesis	4
2 BACKGROUND INFORMATION	5
2.1 Power Plant Modeling and Simulation	5
2.2 Power Plant Model Calibration	6
2.3 Parameter Calibration with Ensemble Kalman Filter	7
2.4 Trajectory Sensitivity Analysis	9
2.5 Recurrence Plots	9
2.6 Orthogonal Projection & Decomposition	10

3	THE PROPOSED COLLINEARITY ANALYSIS METHOD	11
3.1	Introduction	11
3.2	The Power Plant Model	13
3.3	Detection of Sensitive Parameters	16
3.4	The Proposed Collinearity Analysis	16
3.5	Numerical Results	17
3.5.1	Experiment 1	21
3.5.2	Experiment 2	21
3.5.3	Experiment 3	22
3.5.4	Experiment 4	24
3.5.5	Experiment 5	24
3.6	Summary of the Chapter	28
4	THE PROPOSED PARAMETER ERROR IDENTIFICATION METHOD	31
4.1	Introduction	31
4.2	Identifiable Parameter Detection & Grouping	33
4.3	Training Data Creation	34
4.4	CNN Architecture	37
4.5	Erroneous Parameter Identification	37
4.6	Numerical Results	39
4.7	Summary of the Chapter	45
5	CONCLUSION AND FUTURE WORK	47
	REFERENCES	49

LIST OF TABLES

TABLES

Table 3.1	Variable names for the power plant dynamic model.	15
Table 3.2	Parameter Sensitivities for the Bus Fault.	18
Table 3.3	Experiment 1 Results.	21
Table 3.4	Experiment 2 Results.	23
Table 3.5	Experiment 3 Results.	23
Table 3.6	Experiment 4 Results.	24
Table 3.7	Parameter Sensitivities for the Branch Fault.	25
Table 3.8	Experiment 5 Results.	26
Table 4.1	Parameter Sensitivities.	41
Table 4.2	Test 1 Results.	43
Table 4.3	Test 2 Results.	44

LIST OF FIGURES

FIGURES

Figure 2.1	Power plant model calibration by using 'event playback'	7
Figure 3.1	Normalized change in responses (a) P , and (b) Q	11
Figure 3.2	WSCC 9-Bus System	19
Figure 3.3	Collinearity based on P_{sens} for the Bus Fault	20
Figure 3.4	Collinearity based on Q_{sens} for the Bus Fault	21
Figure 3.5	Experiment 1: Estimation of parameter (a) H , (b) K_A , and (c) K_E separately.	22
Figure 3.6	Experiment 2: Estimation of parameter (a) X_d , (b) H , (c) K_E , and (d) K_A simultaneously.	23
Figure 3.7	Experiment 3: Estimation of parameter (a) H , and (b) K_E simultaneously.	24
Figure 3.8	Experiment 4: Estimation of parameter (a) H , and (b) K_E simultaneously when K_A is incorrect.	25
Figure 3.9	Collinearity based on P_{sens} for the Branch Fault	26
Figure 3.10	Collinearity based on Q_{sens} for the Branch Fault	26
Figure 3.11	Experiment 5: Estimation of parameters (a) X_d , (b) H , (c) K_E , and (d) K_A simultaneously.	27
Figure 4.1	Flowchart of the proposed methodology.	32

Figure 4.2	Flowchart of training data generation method.	35
Figure 4.3	Time series power flow data to RP (downsized to 128×128 pixels).	37
Figure 4.4	Flowchart of the proposed method.	40
Figure 4.5	Collinearity Analysis Results.	42
Figure 4.6	Test Case - 1 mismatch decomposition.	43
Figure 4.7	Test Case - 2 mismatch decomposition.	44

LIST OF ABBREVIATIONS

1D	1 Dimensional
2D	2 Dimensional
RP	Recurrence Plots
EnKF	Ensemble Kalman Filter
GE PSLF	General Electric Positive Sequence Load Flow software
PSS/E	Power System Simulator for Engineering software
WSCC	Western Electricity Coordinating Council
API	Application Programming Interface
ANOVA	Analysis of Variance
CNN	Convolutional Neural Network

CHAPTER 1

INTRODUCTION

Calibration of power plant dynamic models is crucial for correct operation and planning of power systems as power systems become more uncertain everyday, due to high penetration of renewable sources and change of behaviour in the demand side [1]. Hence, power plant dynamic models play a more significant role than before for accurate control decision making. During their lifetime, parameters of power plant dynamic models may change due to natural processes and human error. Incorrect dynamic models may create a difference between the actual and simulated power plant response, and hence may cause wrong control decisions, which may lead to serious consequences such as blackouts [2]. In order to prevent such events, power plant dynamic models must be calibrated regularly. Traditionally, power plant dynamic models are calibrated by offline staged tests. However, these tests are considered economically infeasible and unreliable due to being labor intensive, and because of the negative effects of the shutdown of the power plant during the calibration [3]. In recent years, phasor measurement unit (PMU) based online calibration methods are developed as an alternative to traditional offline staged tests [4].

In the literature, there are several approaches for online calibration of power plants based on discrepancy between the actual response and simulated responses of the power plant [4, 5, 6, 7, 8, 9, 10, 11, 12, 13, 14]. PMU at the interconnection of the power plant and the grid records the voltage phasors and the power plant output power flow during a disturbance. Then, those recorded voltage phasors are played back at the interconnection, to decouple the power plant from the rest of the network. This process is called event playback. By utilizing the event playback function, the dynamic model of the power plant is simulated to determine whether the model needs

calibration. The mismatch between the dynamic model response and the actual PMU measurements indicates the existence of erroneous parameters.

Regardless of the parameter calibration technique, most methods apply an identifiability analysis in order to select the identifiable parameters and reduce the size of the calibration problem. Identifiability analysis determines how well the parameters can be estimated from the available PMU measurements. In the literature, sensitivity analyses are used to determine the identifiable parameters in a practical manner. Sensitivity analysis quantifies the relative effect of the parameters on the output. The dynamic power plant model parameters that have a high influence on the electrical power outputs are found as sensitive, hence they are labeled as identifiable parameters. In [4, 7, 9], the trajectory sensitivity analysis is employed and norms of the sensitivity values are used to assess the identifiability. In [12, 13, 14], an analysis of variance (ANOVA) based sensitivity analysis is employed, and the highest ANOVA index is used to determine identifiability before the parameter calibration process. Also, there are other methods for identifiability analysis such as elementary effects method used in [11] which uses the change in the electrical power outputs, and the empirical Gramian based approach is utilized in [10]. These methods are proven to be successful at determining the sensitive parameters, nevertheless, they have similar drawbacks. Firstly, most of the existing methods do not consider the parameter collinearity problem. The collinear parameters cause bias in the calibration process, hence, they must be detected beforehand. Secondly, although possible erroneous parameters are included, the candidate parameter set contains lots of 'distractors' — highly sensitive but already correct parameters[4]. This may bias already correct dynamic model parameters considering the parameter dependence and stochastic calibration processes. Therefore, it is wise to exclude the distractors from the calibration process. [15] and [16] are two pioneer studies which address to decrease the candidate parameter subset further, with more detailed sensitivity analysis metrics by utilizing signal properties of the power plant response. In [15], a systematic approach to advance the traditional sensitivity analysis techniques is presented. In [16], a screening process which utilizes the Hilbert spectrum of previously determined sensitive parameters and model output errors is introduced.

This thesis proposes a method to identify erroneous power plant parameters from

disturbance events by utilizing state-of-the-art CNN classifiers and the orthogonal decomposition technique. The proposed method utilizes the mismatch between simulated dynamic power plant model output power flows and collected PMU measurements from the field during a disturbance. The 1-D time series mismatch data are transformed into 2-D texture images using Recurrence Plots to benefit from promising performance of feature detection of CNN in 2-D signals over 1-D signals [17]. Erroneous parameters are identified from the mismatch via time series image classification using CNN, step by step. Orthogonal decomposition is used to extend the method to multiple parameter error detection. The CNN model is trained with synthetic measurements which are generated by using PSS/E. A trajectory sensitivity analysis is used to determine the most sensitive parameters to decrease the size of the training set. Also, a collinearity analysis method that utilizes trajectory sensitivities is proposed and it is used to group collinear parameters for labeling, which helps to eliminate multiple solutions.

1.1 The Contribution of the Thesis

In the power plant dynamic model calibration problem, the existing methods in the literature include all sensitive parameters to the parameter calibration process. However, the candidate set of parameters to calibrate 1) may not be identifiable due to relation with other parameters in the candidate parameter set, 2) may include already correct parameters and these already correct parameters may effect the accuracy and computation time of the calibration process. This thesis proposes two novel methods to overcome these problems. The contributions of the thesis are as follows;

- 1 - A collinearity analysis method, which detects collinear parameters and prevents multiple solution problem in the power plant dynamic model calibration process, is proposed. The effects of the collinear parameters and the necessity of the proposed method are presented. The fact that sensitivity does not necessarily indicate identifiability is shown with several experiments.
- 2 - A parameter error identification method for power plant dynamic models is proposed. The proposed method identifies the erroneous parameters in the power

plant dynamic model by using the mismatch between the model simulation and the collected PMU measurements at the point of interconnection with the grid.

1.2 The Outline of the Thesis

The thesis is organized as follows; in Chapter 2, the necessary theoretical background on power plant modeling and simulation, power plant model calibration, sensitivity & collinearity analyses, recurrence plots and orthogonal projection & decomposition are given. In Chapter 3, the proposed collinearity analysis method is explained in detail. The method is tested on WSCC 9-bus test system by using the Ensemble Kalman Filter as the parameter estimator. The test results containing all possible cases of collinearity are presented. This chapter proves the necessity of using a collinearity analysis before the calibration process. Chapter 4 presents a novel parameter error identification method for power plant dynamic models. The proposed method identifies the erroneous parameters of a power plant dynamic model by utilizing the PMU measurements at the point of interconnection between the power plant and the grid. The proposed parameter error identification method is also tested on WSCC 9-bus test system with two test cases. In Chapter 5, the thesis is concluded and the future work is given.

CHAPTER 2

BACKGROUND INFORMATION

2.1 Power Plant Modeling and Simulation

Power plants are dynamic systems that are represented by a set of differential algebraic equations. These mathematical equations represent the steady and dynamic states of physical phenomena, and are utilized with the purpose of planning and control. They contain a synchronous generator model (GEN), and usually contain an exciter model (EXC), a governor model (GOV) and a power system stabilizer model (PSS). These subsystems are mathematically coupled with each other, and model a power plant altogether. The dynamic models of power plants are usually provided by the vendor, and they are mostly customer specific. However, with the purpose of data sharing, generic models are developed and utilized widely by parameterizing vendor models. Most commercial power system analysis software provide built-in generic models. The complexity and detail of these models vary, and some models may specialize in specific phenomena such as disturbances, on the other hand, some models are very primitive. In addition to conventional power plants with synchronous generators, the importance of wind turbine generator dynamic models is increased as wind energy becomes a popular renewable energy resource. However, this thesis concerns conventional power plants, and its relation with the dynamic models of wind turbine generators is left as a future work.

Dynamic simulation of power plant models refers to advancing its states from a time instant t to $t + \Delta t$. The time advancement is done by integrating differential equations with respect to time, by using numerical integration methods such as Euler Method. The power plant dynamic model can be reduced to two equations in (2.1) [4].

$$\begin{aligned} dx(t)/dt &= f_c(x(t), u(t), p) \\ y(t) &= h_c(x(t), u(t), p) \end{aligned} \tag{2.1}$$

where x is the state vector, $f(\cdot)$ is the transition function, u is the input vector, p is the power plant parameters, y is the power plant response P_e and Q_e , and $h(\cdot)$ is the output function. Note that c in f_c and h_c denotes continuity.

The states at $t + \Delta t$, $x_{t+\Delta t}$, and the power plant response at $t + \Delta t$, $y_{t+\Delta t}$, depend on the states at t , x_t , the inputs at t , u_t , and the power plant parameters, p . Hence, the states and the power plant response at $t + \Delta t$, $x_{t+\Delta t}$ and $y_{t+\Delta t}$, can be found from integrating the differential equations with respect to time and solving the algebraic equations in (2.1).

2.2 Power Plant Model Calibration

Power plant model calibration is done by a decentralization approach called 'event playback', which is summarized in Fig. 2.1. During a transient event, voltage phasors ($V \angle \theta$) and power flows (P_e , Q_e) are recorded by a PMU located at the interconnection point between the power plant and the rest of the grid. The recorded voltage magnitude and voltage angles are played back at the interconnection point, which models the rest of the grid as an infinite bus. This approach enables simulating any event occurred in the grid back at the power plant, and decouples the power plant dynamics from the network equations. If there is a discrepancy between the simulated power plant output response and measured power flows, the power plant dynamic model is calibrated. The power plant model calibration is done based on the idea of minimizing the mismatch. The dynamic model parameters are calibrated to match the simulated response with measured power flows.

Before the calibration, most methods utilize a sensitivity analysis to with the purpose of determining the identifiable parameters in the dynamic model beforehand. Identifiable parameters are the parameters that are estimable with the existing disturbance data. This is a screening process, where the parameters that are not related to the disturbance are eliminated. This way, the candidate parameter subset to calibrate is

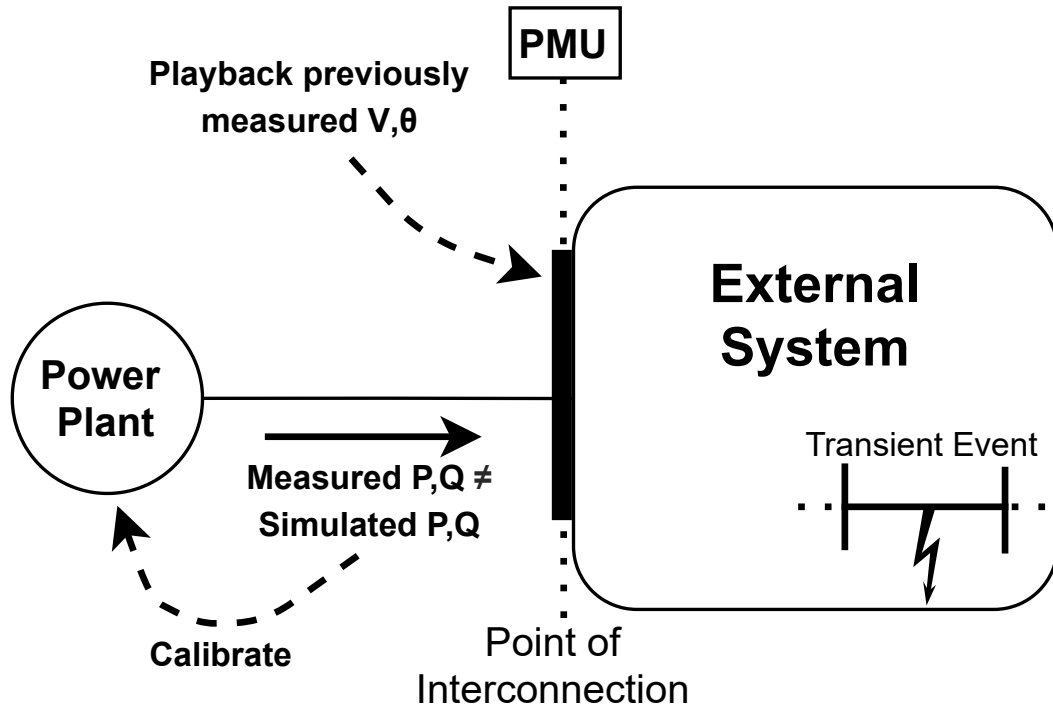


Figure 2.1: Power plant model calibration by using 'event playback'.

decreased.

2.3 Parameter Calibration with Ensemble Kalman Filter

In this thesis, the Ensemble Kalman Filter is employed as the dynamic state and parameter estimator because of its ease of implementation. Nevertheless, the proposed method is applicable to any kind of dynamic state and parameter estimation method since it is independent from the estimator and applied before the estimation process.

The Ensemble Kalman Filter (EnKF) is a Monte Carlo approach for Kalman Filtering that uses a set of state vector samples (ensembles) to sample the covariance matrix. The differential equations constitute the dynamics of the power plant and they are used for constructing the transition function $f(\cdot)$. The algebraic equations constitute the observation function $h(\cdot)$. Thus, the system model can be represented by the following equations.

$$\begin{aligned}
x_k &= f(x_{k-1}, u_{k-1}) + w_{k-1}, w_{k-1} \sim N(\mathbf{0}, Q_{k-1}) \\
\tilde{y}_k &= h(x_k, u_k) + v_k, v_k \sim N(\mathbf{0}, R_k)
\end{aligned} \tag{2.2}$$

where x_k is the vector of system states and u_k is the input vector at time k , w_k and v_k are the zero-mean Gaussian process and measurement noises with covariances of Q_k and R_k respectively.

Priori Step:

$$\begin{aligned}
\hat{x}_k^{-(j)} &= f(\hat{x}_{k-1}^{(j)}, u_{k-1}) + w_{k-1}^{(j)} \\
\hat{x}_k^- &= \frac{1}{N} \sum_{j=1}^N \hat{x}_k^{-(j)} \\
\hat{y}_k^{-(j)} &= h(\hat{x}_k^{-(j)}, u_k) \\
\hat{y}_k^- &= \frac{1}{N} \sum_{j=1}^N \hat{y}_k^{-(j)}
\end{aligned} \tag{2.3}$$

Posterior Step:

$$\begin{aligned}
P^{xy} &= \frac{1}{N} \sum_{j=1}^N (\hat{x}_k^{-(j)} - \hat{x}_k^-)(\hat{y}_k^{-(j)} - \hat{y}_k^-)^T \\
P^{yy} &= \frac{1}{N} \sum_{j=1}^N (\hat{y}_k^{-(j)} - \hat{y}_k^-)(\hat{y}_k^{-(j)} - \hat{y}_k^-)^T \\
K_k &= P^{xy}(P^{yy} + R_k)^{-1} \\
\hat{x}_k^{+(j)} &= \hat{x}_k^{-(j)} + K_k(\tilde{y}_k^{(j)} - \hat{y}_k^-)
\end{aligned} \tag{2.4}$$

In order to estimate the parameter, the state vector x is augmented with the candidate parameters α .

$$x_{aug} = [x \ \alpha]^T \tag{2.5}$$

By augmenting the state vector, the candidate parameters are treated as states. The state vector x is substituted with the augmented state vector x_{aug} where (2.2-2.4) are still valid. The advantage of employing Ensemble Kalman Filter in power plant

model calibration application is the fact that it does not need to calculate the Jacobian matrix. Hence, the analytical model is not needed to be available to the user. The details of the EnKF application on the power plant model calibration problem can be seen in[4].

2.4 Trajectory Sensitivity Analysis

Trajectory sensitivity analysis is a well-known method to obtain local sensitivities of a parameter by calculating the absolute change in the output responses when the parameter is perturbed. The trajectory sensitivities at each time instant are calculated by finite difference approach in (2.6).

$$s_{ki} = \frac{|y(k)|_{\alpha_i + \Delta\alpha_i} - y(k)|_{\alpha_i}|}{|\Delta\alpha_i/\alpha_i|} \quad (2.6)$$

where $y(\cdot)$ active and reactive power flow responses of the power plant, α_i is the power plant model parameter, $\Delta\alpha_i$ is the perturbation on the parameter, $i = 1, 2, \dots, p$ where p is the total number of parameters, and s_{ki} is the local sensitivity of parameter α_i at k^{th} time instant.

Trajectory sensitivity analysis is used to practically determine the identifiable parameters, excluding the collinearity problem. A nonzero sensitivity indicates the existence of influence on the output. Hence, a parameter with nonzero sensitivity is able to change the output. Similarly, a parameter may be identified from the change in the output response, given that the parameter has nonzero sensitivity. In order to determine those parameters, a sensitivity analysis is a necessary tool before the parameter calibration process. Note that, the parameter sensitivities usually increase with the severity of the transient event.

2.5 Recurrence Plots

Recurrence Plots (RP) is a technique which efficiently visualizes recurrences of a trajectory $\vec{x}_i \in \mathbb{R}^d$ in phase space as a square matrix. Recurrence occurs when a

trajectory visits approximately the same state, i.e. $\vec{x}_i \approx \vec{x}_j$, at time instants i and j . These recurrence are stored in \mathbf{R} , recurrence matrix, whose formal expression is given below.

$$\mathbf{R}_{i,j}(\varepsilon) = \Theta(\varepsilon - \|\vec{x}_i - \vec{x}_j\|) \quad (2.7)$$

where $i, j = 1, \dots, N$, N is the total time instants, ε is a threshold distance, $\Theta(\cdot)$ is the Heaviside function where $\Theta(x) = 0$ if $x < 0$, and $\Theta(x) = 1$ otherwise, and $\|\cdot\|$ is a norm. The RP visualizes the time instants when system states approximately recur. The recurrences are indicated in \mathbf{R} by $\mathbf{R}_{i,j} = 1$, and plotted in RP with black dots at coordinate i and j . In the absence of recurrence $\mathbf{R}_{i,j} = 0$ and corresponding coordinates have white dot. More details on the theoretical background of RP can be found in [18]. Note that, threshold distance, ε , is taken as zero in the proposed method.

2.6 Orthogonal Projection & Decomposition

A vector u in \mathbb{R}^n can be written as sum of two orthogonal vectors, $u = w + w^\perp$, where w is orthogonal projection of u onto another vector v in \mathbb{R}^n ($proj_v u$), and w^\perp is its complement. The complement of the orthogonal projection of u onto v , which corresponds to the perpendicular component of u with respect to v , is shown below.

$$w^\perp = u - proj_v u = u - \frac{u \cdot v}{\|v\|^2} \cdot v \quad (2.8)$$

The orthogonal decomposition is used to enable the proposed method to identify multiple parameter errors by eliminating the individual effect of the erroneous parameters from the mismatch between the collected measurements and the power plant response.

CHAPTER 3

THE PROPOSED COLLINEARITY ANALYSIS METHOD

3.1 Introduction

This thesis proposes an identifiability analysis that combines the well-known trajectory sensitivity analysis with collinearity analysis. The utilization of the sensitivities of the parameters in time enables us to assess their collinearity relations[19]. Thanks to this, the parameter selection process is enhanced by separating the candidate parameters into groups considering their collinearities as well as their sensitivities instead of only taking the sensitivities into account. Hence, the potential bias created by the linear dependency is avoided. Note that, the proposed method is an estimator independent method such that it can be used before any estimator without any alteration.

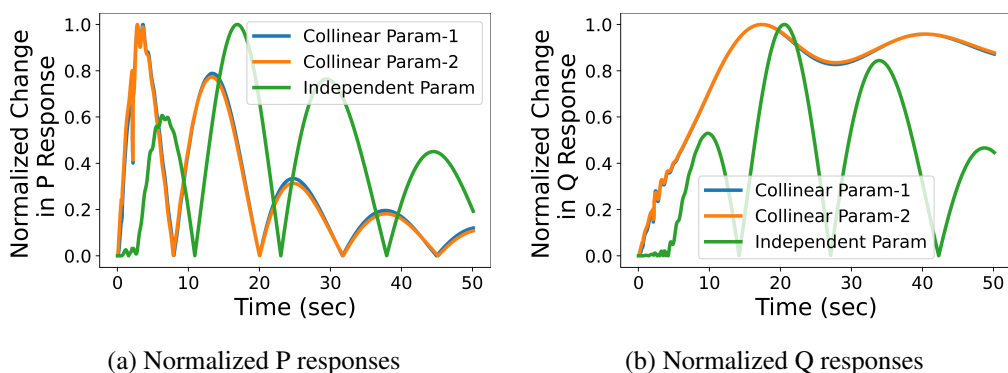


Figure 3.1: Normalized change in responses

(a) P , and (b) Q .

Selection of a set of candidate parameters plays a very important role in parameter

estimation. An appropriate set of candidate parameters are selected according to their sensitivity. Note that, the identifiability and the sensitivity are related in the dynamical systems [20]. Hence, by analysing the sensitivities, the identifiability of the parameters can be inspected. High sensitivity indicates the high level of information about the parameter and is required for a good quality estimation. Hence, the parameters with the low sensitivity values are screened out to eliminate the insensitive parameters which are not identifiable.

The sensitivities of the parameters along the trajectory can give extra information such as the linear dependency with other parameters. Fig.3.1 shows the normalized change in the output responses of the power plant for equal percentage of perturbation on each of the three parameters and the actual output responses, which later will be used in sensitivity calculations. In other words, it shows the effects of perturbation on the output response for each parameter. It can be deduced that the collinear parameters have the same effect on the normalized output response for the same proportion of perturbation which will reflect on their trajectory sensitivities. In the employed power plant model, the collinear parameters correspond to K_A and K_E , and the independent parameter corresponds to H . It is obvious that those collinear parameters cannot be identified from their output responses without further information, on the other hand, since the independent parameter has a very different output response, it is identifiable. In order to utilize this information, the sensitivity matrix is constructed out of the sensitivities in time. The rank of the sensitivity matrix indicates the identifiability of the parameters. The full rank sensitivity matrix means that all of the parameters are identifiable where the singular sensitivity matrix means that there is at least one parameter which is not identifiable[21]. Moreover, the sensitivity matrix is used to extract the information of linear dependency between the parameters. In[22], the authors proposed to rank the columns of sensitivity matrix corresponding to the parameters using an orthogonal-projection based method. However, it does not give the collinearity information explicitly. In[19], a collinearity index is proposed that includes the multiple calculation of eigenvalues which is computationally expensive. This method utilizes *cosine* similarity to obtain the collinearity level of the parameters. Parameters with *cosine* similarity close to 1 are determined as the highly collinear parameters. These parameters have the same effect on the output.

Thus, they are no longer identifiable together and not jointly estimated. The method successfully detects the collinear parameters among the selected subset of sensitive parameters before the estimation. Hence, the estimation bias which occurs due to the collinearity is avoided.

The proposed method relies on the trajectory sensitivity analysis as it provides the sensitivity of the parameters along the trajectory. Since the sensitivity is interchangeable with identifiability in dynamic systems, the trajectory sensitivity analysis provides sufficient information to select the best appropriate subset of candidate parameters. The sensitivity analysis is divided into two steps, namely the detection of sensitive parameters and the collinearity analysis.

3.2 The Power Plant Model

The dynamic response of the power plants can be formulated with a set of nonlinear differential and algebraic equations. These equations drive the states of the system in time. Although the proposed method is applicable to widely used simulation softwares, such as GE PSLF and PSS/E, in this study, the two-axis model is used to model the power plant with a synchronous generator, a IEEE DC1A type exciter and, TGOV1 type turbine-governor from [23] for sake of simplicity, which is also employed in [24] and [25]. The the power plant model is given below, and the related variable names are given in Table 3.1.

Synchronous Generator:

$$T'_{do} \frac{E'_q}{dt} = -E'_q - (X_d - X'_d)I_d + E_{fd} \quad (3.1)$$

$$T'_{qo} \frac{E'_d}{dt} = -E'_d - (X_q - X'_q)I_q \quad (3.2)$$

$$\frac{d\delta}{dt} = \omega - \omega_s \quad (3.3)$$

$$\frac{2H}{\omega_s} \frac{d\omega}{dt} = T_M - P_e - D(\omega - \omega_s) \quad (3.4)$$

IEEE DC1A Exciter:

$$T_E \frac{dE_{fd}}{dt} = -(K_E + S_E(E_{fd}))E_{fd} + V_R \quad (3.5)$$

$$T_F \frac{dR_f}{dt} = -R_f + \frac{K_F}{T_F} E_{fd} \quad (3.6)$$

$$T_A \frac{dV_R}{dt} = -V_R + K_A \left(R_f - \frac{K_F}{T_F} E_{fd} + V_{ref} - V_t \right) \quad (3.7)$$

IEEE TGOV1 Turbine-Governor:

$$T_{CH} \frac{dT_M}{dt} = -T_M + P_{SV} \quad (3.8)$$

$$T_{SV} \frac{dP_{SV}}{dt} = -P_{SV} + P_C - \frac{1}{R_D} \left(\frac{\omega}{\omega_s} - 1 \right) \quad (3.9)$$

Network Equations:

$$V_d = V \sin(\delta - \theta), V_q = V \cos(\delta - \theta), \quad (3.10)$$

$$I_d = \frac{E'_q - V_q}{X'_d}, I_q = \frac{V_d - E'_d}{X'_q} \quad (3.11)$$

$$P_e = V_d I_d + V_q I_q, Q_e = -V_d I_q + V_q I_d, \quad (3.12)$$

A decentralized approach (event playback) is obtained by replaying the measured V and θ , as the real and reactive electrical power output can be calculated using only the differential algebraic equations of the power plant.

Table 3.1: Variable names for the power plant dynamic model.

Variable symbol	Variable name
E'_q, E'_d	q-axis and d-axis transient voltages
δ	Rotor angle
ω, ω_s	Rotor speed and synchronous speed
E_{fd}	Exciter output voltage
R_f	Rate feedback
V_R	Regulator output voltage
T_M	Scaled mechanical torque to the shaft
P_{SV}	Steam valve position
P_C	Control input
X_d, X_q	d and q axis synchronous reactances
X'_d, X'_q	d and q axis transient reactances
T'_{do}, T'_{qo}	d and q axis transient open circuit time constants
T_E	Exciter time constant
T_F	Regulator stabilizing circuit time
T_A	Regulator amplifier time constant
T_{CH}, T_{SV}	Turbine-Governor time constants
H	Generator inertia
D	Damping constant
K_A	Regulator gain
K_E	Exciter constant related to self-excited field
K_F	Regulator stabilizing circuit gain
S_E	Exciter saturation function
R_D	Speed regulation quantity
V_{ref}	Regulator reference voltage setting
V, θ	Terminal bus voltage magnitude and voltage angle
I_d, I_q	Stator d-axis and q-axis currents
P_e, Q_e	Real and reactive electrical outputs.

3.3 Detection of Sensitive Parameters

In order to construct the sensitivity matrix, the approximate local sensitivities of the parameters at each time instant is calculated by finite difference approach in (3.13).

$$s_{ki} = \frac{|y(k)|_{\alpha_i + \Delta\alpha_i} - y(k)|_{\alpha_i}|}{|\Delta\alpha_i/\alpha_i|} \quad (3.13)$$

where $y()$ is the real or reactive power output function of the power plant, α_i is the candidate parameter, $\Delta\alpha_i$ is the small perturbation to the parameter and $i = 1, 2, \dots, p$ where p is the number of parameters. The i_{th} column of the sensitivity matrix S in (3.14) is filled with sensitivity value of the parameter α_i at each time step k . Note that, both the real and reactive power sensitivity matrices are constructed in this step.

$$S = \begin{bmatrix} s_{11} & \cdot & s_{1i} & \cdot & s_{1p} \\ s_{21} & \cdot & s_{2i} & \cdot & s_{2p} \\ \vdots & \vdots & \vdots & \vdots & \vdots \\ s_{k1} & \cdot & s_{ki} & \cdot & s_{kp} \end{bmatrix} \quad (3.14)$$

The columns of the sensitivity matrix S corresponds to the parameters of the model. The ℓ_1 norms of the columns give insight about the identifiability of the parameters. The parameters corresponding to the zero or very small norms in both of the sensitivity matrices are unidentifiable parameters. They are eliminated from the candidate parameters list, and the columns of S corresponding to those parameters are removed from the matrices. The rest are the sensitive ones.

3.4 The Proposed Collinearity Analysis

Although some highly sensitive parameters are estimable one by one, the simultaneous estimation quality becomes poorer as the collinearity between the parameters increases. Even more, the estimation results may be biased when one of the two incorrect and collinear parameters is estimated separately. The columns with strong linear dependency cause singularity in the sensitivity matrix S , which is an indicator

of collinearity between the parameters. Hence, the collinear parameters should be identified. Otherwise, their simultaneous estimation may be biased.

The collinearity analysis is done using the *cosine* similarity principle. The *cosine* similarity principle quantifies the linear dependency between two vectors between 0 and 1. It reveals the cosine of the angle between the vectors, and reveals if those vectors are roughly in the same direction[26]. Note that, each column of the sensitivity matrix S corresponds to the parameter sensitivities along the trajectory. Therefore, those columns will be used to assess the collinearities. The *cosine* similarity formulation is given in (3.15).

$$\cos\theta_{ij} = \frac{v_i \cdot v_j}{\|v_i\| \|v_j\|} \quad (3.15)$$

where v_i and v_j are the columns of S corresponding to i_{th} and j_{th} parameters, and θ_{ij} is the angle between v_i and v_j .

The sensitivity vectors of the parameters which have *cosine* similarity close to 1 show very strong linear dependency. By this means, the collinear parameters are determined.

3.5 Numerical Results

In this section, a study case will be presented using the WSCC 9-Bus System shown in Fig. 3.2 [27]. The power plant of interest is modeled with the power plant model presented in Chapter 3.2. A study case is created by applying a symmetrical 3-phase fault at the terminals of the power plant. The response of the power plant is recorded, and Gaussian noise is added to obtain synthetic PMU measurements. Note that, different cases with different transient types can also be created.

First, the trajectory sensitivity analysis in (3.13) is carried out for all of the parameters and the sensitivity matrix S given in (3.14) is constructed. The Table 3.2 shows the sensitive parameters and their sensitivity values which are the ℓ_1 norms of the columns.

Table 3.2: Parameter Sensitivities for the Bus Fault.

Parameter	P sensitivity	Q sensitivity
X_d	2.1420	2.9558
X'_d	0.4421	0.4880
X_q	0.4897	0.2728
X'_q	0.1217	0.0880
T'_{do}	0.2796	0.2920
T'_{qo}	0.0456	0.0225
H	1.3801	0.4563
D	0.0011	0.0004
K_E	2.0631	3.1967
T_E	0.0924	0.0664
S_E	0.1315	0.2039
K_A	2.2552	3.4343
K_F	0.6099	0.4319
T_F	0.3182	0.1844
T_A	0.0633	0.0453
T_{SV}	0.0005	0.0002
T_{CH}	0.0009	0.0004
R_D	0.0076	0.0023

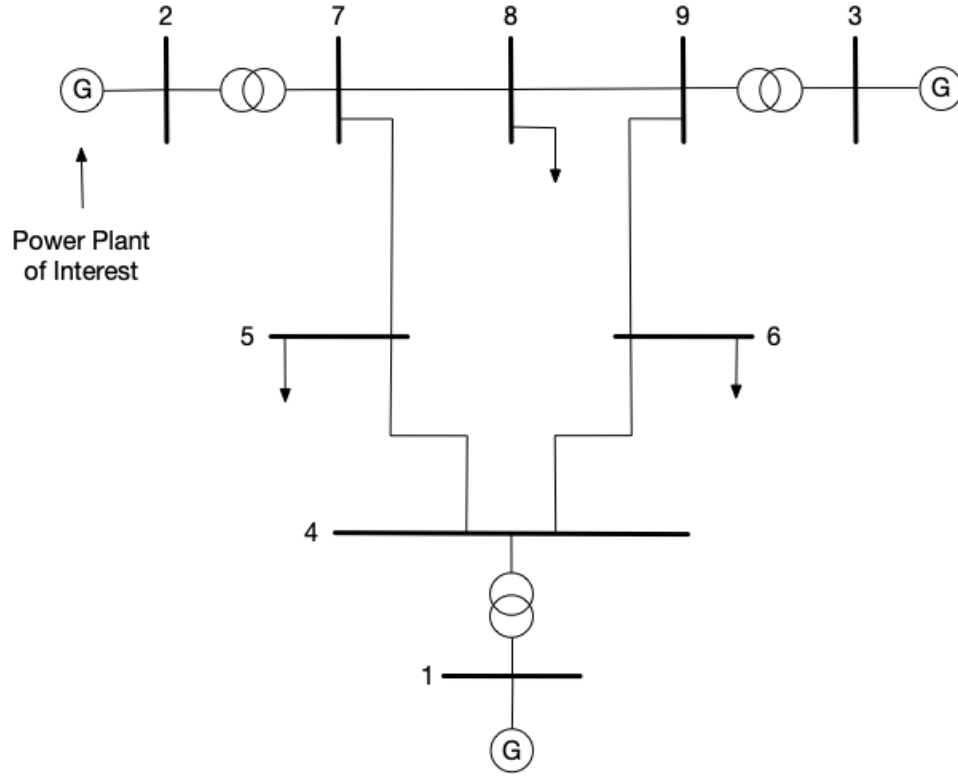


Figure 3.2: WSCC 9-Bus System

The parameters X_d , H , K_E , and K_A are found to be the most sensitive parameters to the applied transient. Therefore, those parameters are utilized in the demonstration experiments in the rest of the chapter, although the parameters with nonzero ℓ_1 norm are identifiable as well. Hence, only the columns corresponding to these four parameters are left in the sensitivity matrix S . Then, the *cosine* similarities of the columns corresponding to those parameters are obtained by (3.15). Fig. 3.3 and 3.4 show the *cosine* similarities of the parameters based on their columns in the sensitivity matrices. It is found that the linear dependency of X_d , K_E and, K_A are significantly high. On the other hand, H is clearly independent from the other parameters. Therefore, in an optimally selected subset of parameters for estimation, only one parameter among X_d , K_E and, K_A should exist along with H . Note that instead of making this decision based on the highest ℓ_1 norm value in the sensitivity matrix, it is more suitable to use engineering judgement since all of the parameters are already highly sensitive. Note that, inclusion of a parameter with collinear relations may be problematic in any case as the estimation may be biased because of error in the other collinear parameters.

Note that, these numerical results are specific to the 3-phase fault at the terminals of the power plant. Sensitivity of the parameters may change based on the severity and the type of the transient event, as the output response of the power plant may not be the same for the same amount of perturbation on a parameter. Whilst some parameters may not participate in a certain disturbance, they may dominate the output on another. This fact is reflected on (3.13) such that the amount of the change in the output may result a change in the sensitivity in time. That being said, collinearity relations of parameters may not remain the same for different event types by means of the change in the sensitivities. Moreover, different dynamics of the grid such as switching time may have an effect on the collinearity considering more complex models involving saturation effects. It is also noteworthy to emphasize that the collinearity between parameters may be the result of mathematical expressions. Such structural collinearities make the collinear parameters structurally unidentifiable and cannot be eliminated. Regardless of the type, any disturbance can be simulated by utilizing the playback signals at the point of interconnection, and the rest of the analysis steps can be applied without loss of generality. The proposed method does not depend on disturbance types, while the results may.

X_d	1.0	0.72	0.992	0.994
H	0.72	1.0	0.65	0.668
K_E	0.992	0.65	1.0	0.999
K_A	0.994	0.668	0.999	1.0
	X_d	H	K_E	K_A

Figure 3.3: Collinearity based on P_{sens} for the Bus Fault

The effect of the collinearity in the estimation is shown via five different experiments which are presented below.

X_d	1.0	0.102	0.997	0.998
H	0.102	1.0	0.133	0.124
K_E	0.997	0.133	1.0	0.999
K_A	0.998	0.124	0.999	1.0
	X_d	H	K_E	K_A

Figure 3.4: Collinearity based on Q_{sens} for the Bus Fault

3.5.1 Experiment 1

In this experiment H , K_E and, K_A are included in the augmented state vector in (2.5) separately, i.e. the parameters are included to the state vector one by one, and three different estimations are conducted. Fig. 3.5 shows their trajectories in time. All three parameters are converged to their true values provided that all parameters that are not estimated are correct, which was expected since all three are highly sensitive and, there does not exist any collinearity relation.

Table 3.3: Experiment 1 Results.

Parameter	Initial	After calibration	True
H	10	6.399	6.4
K_A	25	19.993	20
K_E	0.6	1.000	1

3.5.2 Experiment 2

In this experiment X_d , K_E and K_A , which are determined as highly sensitive parameters but have collinearity among them, and H are simultaneously estimated. Fig. 3.6

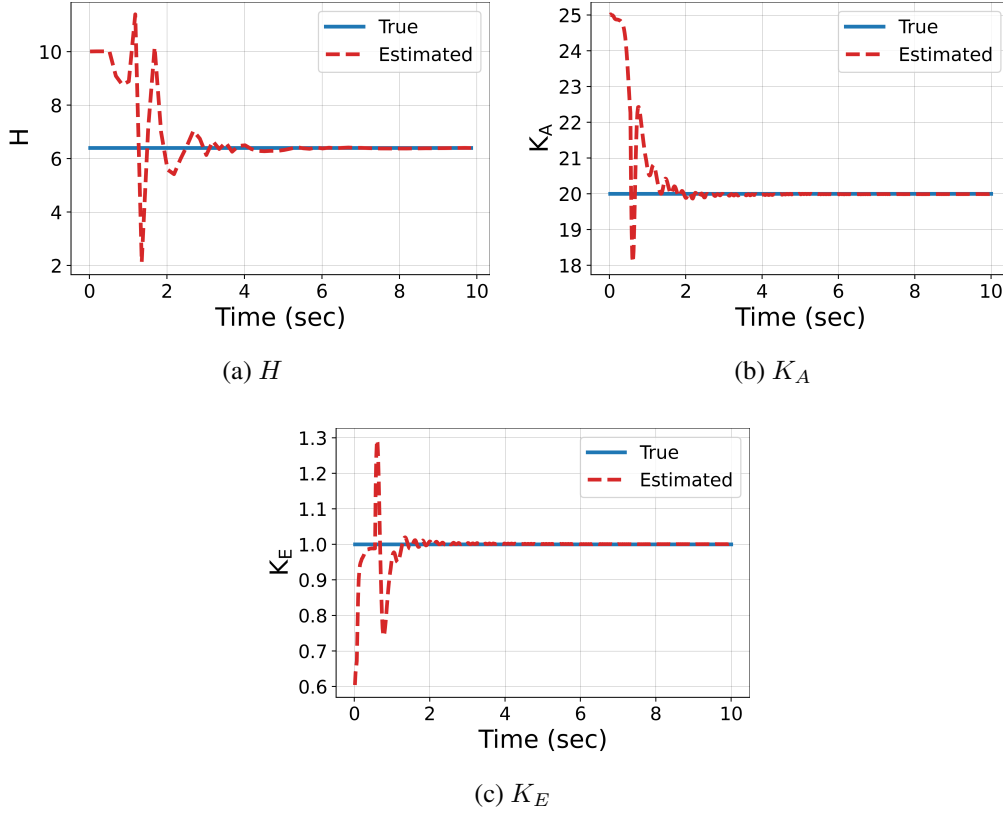


Figure 3.5: Experiment 1: Estimation of parameter (a) H , (b) K_A , and (c) K_E separately.

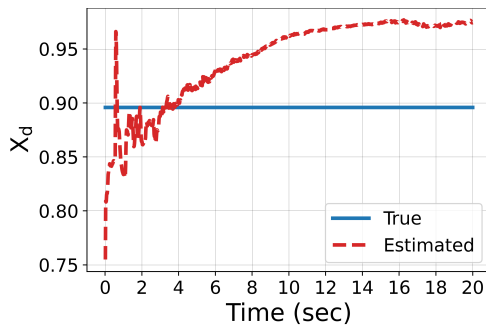
shows that the effect of the collinearity on the estimation. Although all parameters are highly sensitive, the estimation result is biased because of the collinearity between three parameters. The *cosine* similarity between X_d , K_E and K_A are very close to 1 for both P and Q trajectory sensitivities, therefore, these parameters were not able to be identified correctly. However, H is estimated successfully since it does not have high collinearity.

3.5.3 Experiment 3

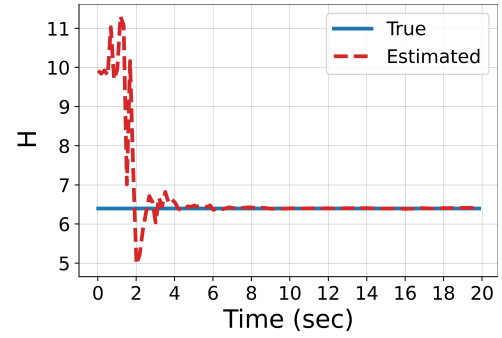
In this experiment H and K_E , which are determined as highly sensitive parameters and do not have collinearity among them, are simultaneously estimated. Fig. 3.7 shows that H and K_E can be simultaneously estimated successfully.

Table 3.4: Experiment 2 Results.

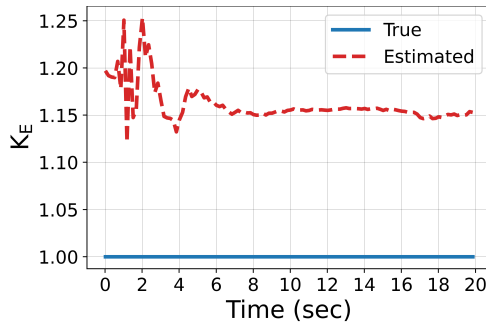
Parameter	Initial	After calibration	True
X_d	0.7632	0.9754	0.8958
H	10	6.427	6.40
K_E	1.2	1.155	1
K_A	25	24.57	20



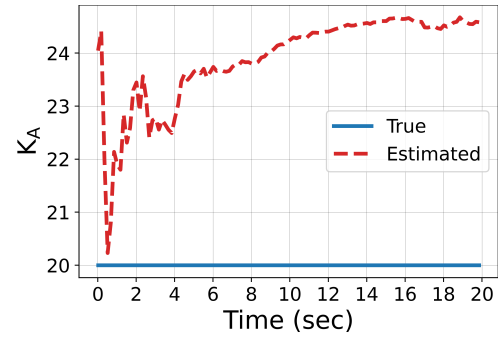
(a) X_d



(b) H



(c) K_E



(d) K_A

Figure 3.6: Experiment 2: Estimation of parameter (a) X_d , (b) H , (c) K_E , and (d) K_A simultaneously.

Table 3.5: Experiment 3 Results.

Parameter	Initial	After calibration	True
H	10	6.397	6.4
K_E	0.6	1.00	1

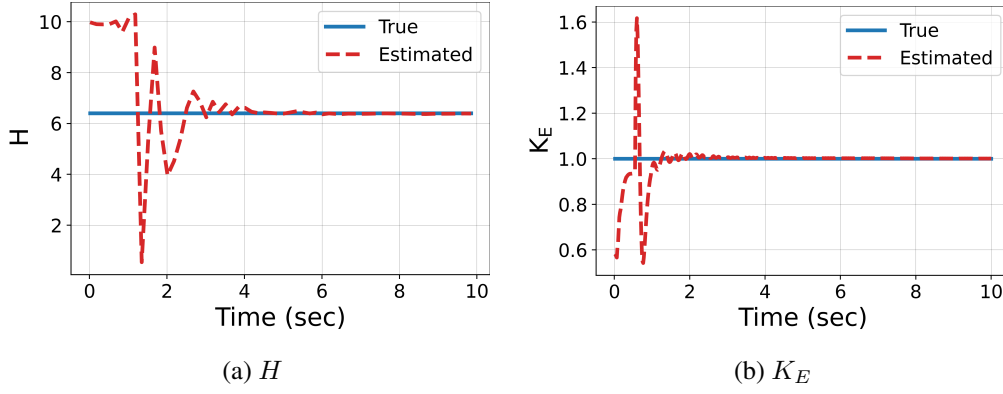


Figure 3.7: Experiment 3: Estimation of parameter (a) H , and (b) K_E simultaneously.

3.5.4 Experiment 4

In this experiment H and K_E , which are determined as highly sensitive parameters and do not have collinearity among them, are simultaneously estimated while K_A is intentionally biased before the estimation. Fig. 3.8 shows that while the independent parameter H can be estimated successfully, the estimation result of K_E is incorrect.

Table 3.6: Experiment 4 Results.

Parameter	Initial	After calibration	True
H	10	6.405	6.4
K_E	0.6	1.268	1

3.5.5 Experiment 5

In this experiment, another study case is created by applying symmetrical 3-phase fault at the middle of the transmission line between buses 4 and 6, and synthetic PMU measurements are obtained. A sensitivity analysis is carried out and the most sensitive parameters are found as X_d , H , K_E , and K_A . The results of the sensitivity analysis are shown in Table 3.7. Then, the proposed collinearity analysis method is applied. The *cosine* similarities are shown in Fig. 3.9 and Fig. 3.10. For this disturbance, the collinearity of X_d between K_E , and K_A with respect to real power is decreased.

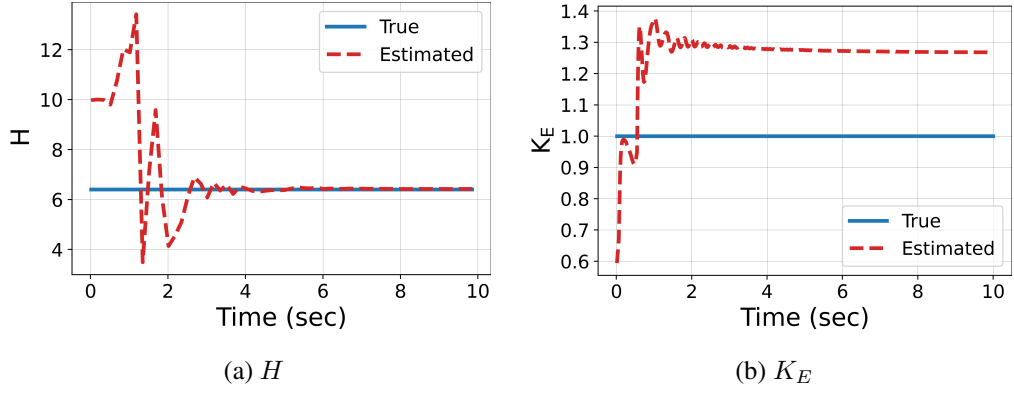


Figure 3.8: Experiment 4: Estimation of parameter (a) H , and (b) K_E simultaneously when K_A is incorrect.

However, the collinearity between K_E and K_A remained the same as expected since they are structurally collinear in this power plant model. Fig. 3.11 shows that the parameters H and X_d are estimated successfully as they have high sensitivity and have *cosine* similarity far away from 1. However, the estimation results of K_E and K_A are again biased because of their collinearity.

Table 3.7: Parameter Sensitivities for the Branch Fault.

Parameter	P sensitivity	Q sensitivity
X_d	0.4993	1.9382
H	0.2311	0.2050
K_E	0.5305	2.7633
K_A	0.5759	2.916

The trajectory sensitivity analysis successfully identified the parameters with high sensitivity, while the proposed method revealed the collinearity among those sensitive parameters. Despite the successful estimation of the parameters H , K_A and, K_E separately provided that the other parameters are correctly known, simultaneous estimation of the parameters may not give the same result due to collinearity between the parameters K_A and K_E even if the other parameters were correct. In the considered model, the collinearity arises from (3.5) and (3.7) in which those parameters are in

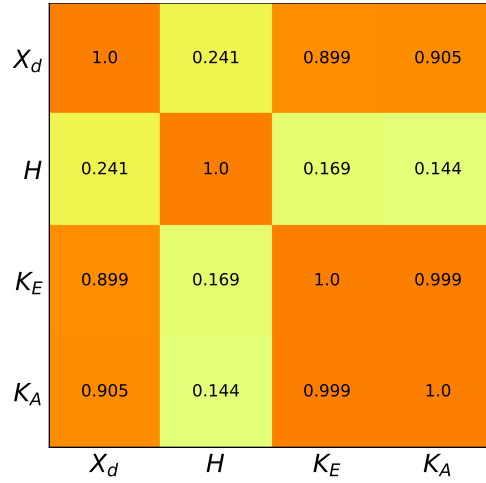


Figure 3.9: Collinearity based on P_{sens} for the Branch Fault

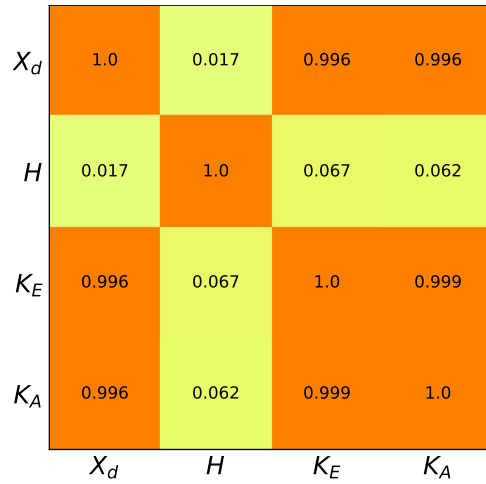


Figure 3.10: Collinearity based on Q_{sens} for the Branch Fault

Table 3.8: Experiment 5 Results.

Parameter	Initial	After calibration	True
X_d	0.7632	0.8953	0.8958
H	10	6.4099	6.4
K_E	1.2	1.1111	1
K_A	25	22.0831	20

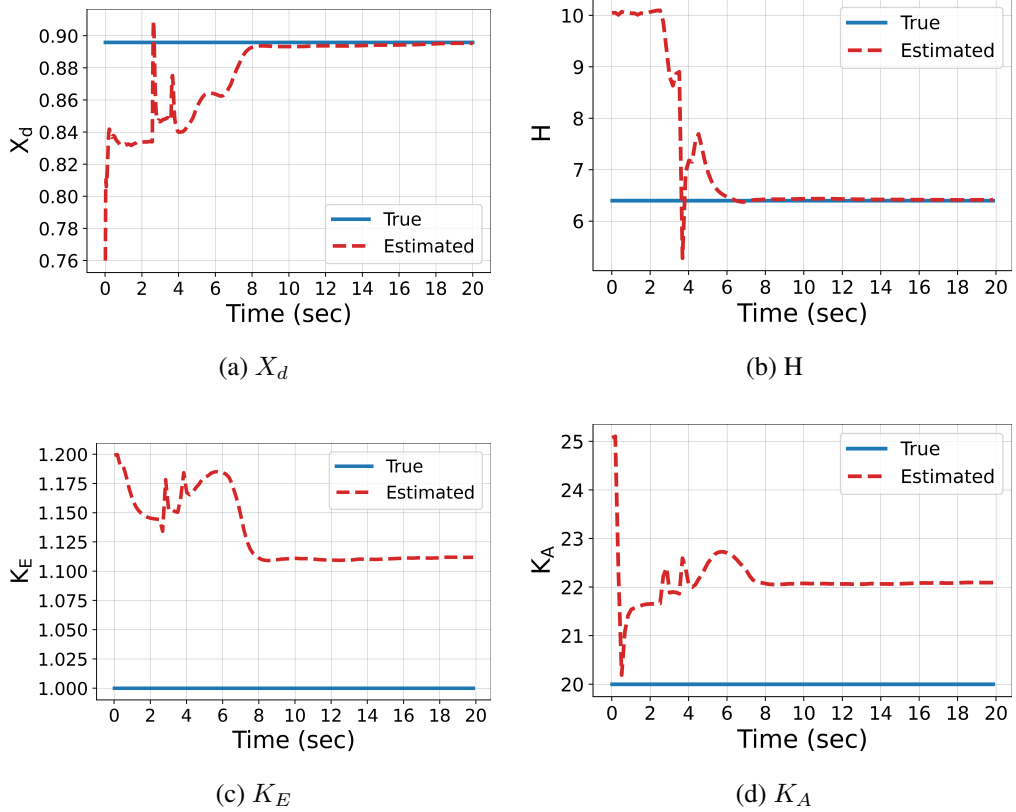


Figure 3.11: Experiment 5: Estimation of parameters (a) X_d , (b) H , (c) K_E , and (d) K_A simultaneously.

the form of multiplication. During the estimation, the parameters are assigned to the values whose ratio is close to the ratio of the true values of the parameters. Hence, the bias may not be apparent to the event playback of other transient cases with the resultant parameters from this biased estimation. If there is suspicion about the values of collinear parameters, and the collinearity cannot be removed by any method, the authors recommend offline staged tests instead of online parameter calibration as corruption in one of two collinear parameters may cause bias on the other.

The numerical results show that in the presence of high collinearity in the subset of highly sensitive parameters, the estimation is of poor quality. The linear dependency of the parameters make them unidentifiable. Moreover, Experiment 5 shows that some parameters, such as X_d , have event specific collinearity between other parameters and they can be estimated by utilizing different type of disturbances, and some parameters such as K_E and K_A are unidentifiable by structure. Therefore, it is shown

that the collinearity analysis is a necessity after the sensitivity analysis.

3.6 Summary of the Chapter

The parameter selection process is very crucial in dynamic parameter estimation. It directly affects the performance of the estimator. Hence, selecting the best subset of the parameters is an important task. Selection of the parameters is done according to the sensitivity analysis as sensitivity is related with identifiability. Although the detection of highly sensitive parameters is very important, it is not sufficient to check the sensitivity solely as high sensitivity does not always mean strong identifiability because of the parameter relations in the model. In dynamic systems, observability is a time-dependent problem where the sensitivity of the states and parameters change within time. Apart from the identifiability of the parameters, the relation between the parameters can be extracted from the trajectory sensitivities, since the effect of the collinear parameters on the output will be similar. Hence, collinearity can be assessed from the sensitivity values over time. This chapter proposes to use *cosine* similarity method to identify the collinear parameters after the trajectory sensitivity analysis by utilizing this fact. This chapter shows that the traditional sensitivity analyses provide missing information on the identifiability of the power plant parameters in the presence of collinear parameters. Although some parameters are highly sensitive, their estimates may be biased. The proposed method determines the collinear parameters in the candidate parameter set, and warns the operator about the potential bias in the estimates of those parameters.

Numerical results proved the necessity of the collinearity analysis in the dynamic parameter estimation problem. In the presence of sensitive and linearly independent parameters in the augmented state vector, the parameter estimation could be performed with a good accuracy. On the other hand, the presence of sensitive but collinear parameters in the augmented state vector caused bias in the estimates of those parameters. Hence, without the collinearity analysis, the estimation result may be biased for the linearly dependent parameters in the model. In addition to these, with the help of the proposed collinearity analysis, it is shown that the collinearity of some parameters may change with respect to the severity/type of the disturbances. The proposed

method provides a very effective decision support for the optimum utilization of the disturbance measurements. It pre-processes the disturbance data with the power plant model and help the operator to avoid biases arising from collinearity of the parameters. It provides a critical advice to the operator about identifiability of the parameters from the available and scarce data.

Note that, while the quality of simultaneous estimation is poor in the presence of collinear parameters, the separate estimation may also be poor in some cases. For example, when one of two collinear parameters are corrupted and deviated from its true value, the estimation of the other parameter also becomes corrupted. It is shown that the identification of the collinear parameters are very problematic, and in some cases impossible. Hence, authors recommend offline staged tests or using additional disturbance data if there is not enough information about the present values of collinear parameters.

CHAPTER 4

THE PROPOSED PARAMETER ERROR IDENTIFICATION METHOD

4.1 Introduction

This thesis proposes a method to identify multiple inaccurate power plant parameters based on the mismatch between the power plant model response and collected PMU measurements by using time series image classification with CNN and orthogonal decomposition. The proposed method is applied to a selected disturbance event, and its aim is to identify erroneous parameters by using the selected event data and the simulated dynamic model response.

Traditional methods usually only utilize ℓ_1 norm of local sensitivities of power plant parameters to determine the subset of candidate parameters for calibration. Naturally, all parameters which have an influence on the power plant output response are determined as sensitive parameters. Hence, most of them are included in the calibration process, and they are treated as potentially erroneous. As being sensitive does not necessarily mean being erroneous, the set of sensitive parameters may include already calibrated parameters, which may cause performance loss.

Power plants are modeled with nonlinear differential algebraic equations. These models are very complex, and represent the dynamic behaviour of power plants. A change in a parameter of the model may not change the magnitude of the output merely, it may also change other properties of its transient response such as delay time, settling time and peak time. Error on each sensitive parameter contributes to the output response mismatch by changing those specific characteristics of the output response. The proposed method utilizes those changes in the output response in order to identify the erroneous parameters.

For a selected disturbance event, first, identifiable parameters are detected by using trajectory sensitivity analysis, and collinear parameters are determined by using the results of the sensitivity analysis. Then, the sensitive parameters are grouped based on the collinearity analysis results. The groups are called *Class* in this thesis. A training dataset that contains the mismatches is synthetically generated by biasing the available values of the sensitive parameters of the model, i.e. by applying perturbation, one by one. The mismatches are obtained by subtracting the biased output response of the power plant from its bias-free response. In the dataset, each mismatch is labeled with respect to the *Class* of its corresponding biased parameter. The training set is converted into 2-D images from 1-D time series signals with the help of RP. The CNN model is trained with the 2-D time series images and corresponding labels. Finally, a recursive algorithm which identifies the erroneous parameters is applied by utilizing the CNN model and orthogonal projection. The flowchart in Fig. 4.1 summarizes the general process.

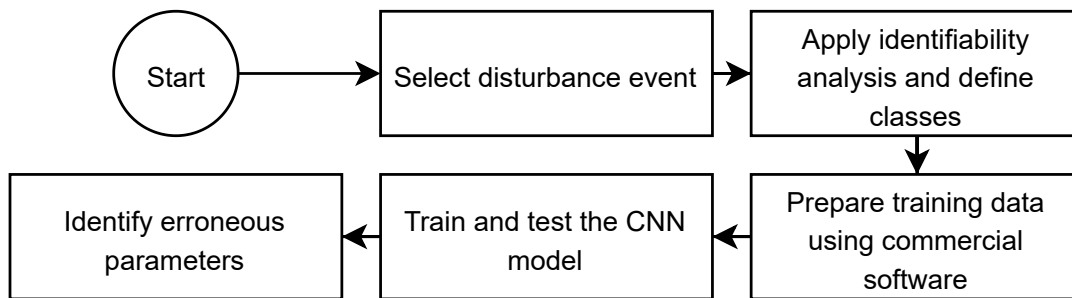


Figure 4.1: Flowchart of the proposed methodology.

The training data could be easily generated by using commercial software, such as PSS/E. Note that, the training data is synthetically generated with the available dynamic model. Hence the proposed method does not use real disturbance data to train the CNN.

The proposed method has several advantages over a classical multi-label classifier, i.e. the classifier that is trained with the mismatch data of multiple biased parameter combinations. First, the proposed method does not need training data with every bias combination. The training data contain mismatches caused by only a single biased parameter at each time, which decreases the training data generation and model training times significantly. Moreover, a biased parameter may not always be identified

from the mismatch directly due to having relatively smaller effect on the mismatch. That is to say, in a case where two parameters are biased, bias on a highly sensitive parameter may dominate the mismatch such that the bias on a parameter with low sensitivity may not contribute to the mismatch as much. In that case, the individual mismatch created by the bias on the highly sensitive parameter and the mismatch created by combination of the two parameters would be similar. Nevertheless, they would be labeled differently. Consequently, it may degrade the performance of the classifier. That being said, a training set with the mismatch data including multiple biased parameter combinations could be an alternative if a more advanced classifier is implemented. However, the proposed method is already able to identify the erroneous parameters step-by-step which requires the CNN to identify one erroneous parameter at a time, thanks to the elimination of the effect of the identified erroneous parameters on the mismatch.

4.2 Identifiable Parameter Detection & Grouping

As the first step, an identifiability analysis is performed by using the well-known trajectory sensitivity analysis in order to determine the possible erroneous parameters. Note that, only the significantly sensitive parameters have influence on the output. Therefore, only the parameters that are both sensitive and erroneous are responsible for the mismatch. Consequently, the subset of sensitive parameters contains the erroneous parameters if there is any. On the other hand, this does not mean that non-sensitive parameters may not have errors. As the nonsensitive parameters do not have any influence on the output for considered disturbance, it is not possible to detect the existence of error on them. Hence, they are removed from the erroneous parameter detection problem. However, it is possible to use another disturbance data where nonsensitive parameters for a certain disturbance are highly sensitive. For a selected disturbance, trajectory sensitivity analysis in (3.13) is applied, and sensitivity matrix S in (3.14) is constructed. Parameters with zero sensitivity are eliminated.

Collinear parameters cause a great threat to accuracy of both calibration and erroneous parameter identification processes. Since the collinear parameters have similar influence on the output response of the power plant, they can not be identified from

their output response. Thus, although the collinear parameters might have high sensitivity, we can not identify which one of the collinear parameters has error if one of them is corrupted without additional data. Therefore, before the classification these collinear parameters are detected via *cosine* similarity method using S . Nevertheless, though the fact that which of the collinear parameters has the error can not be determined, it is possible to localize the parameter with error by grouping the collinear parameters. In this way, accuracy of classifiers increase, and potential bias is eliminated. Each group of collinear parameters are labeled as a *Class* for the classification.

4.3 Training Data Creation

In order to train the CNN model, an adequate sized and properly arranged training data is necessary. In this step, commercial software which have dynamic analysis simulation tools such as PSS/E and GE PSLF could be taken advantage of. With the help of Application Programming Interface (API) of these commercial software, necessary data could be created in Python environment easily.

The proposed method utilizes the mismatch between the power plant model response and the actual measurements from the field, which is caused by the parameter errors on the model. The mismatch is a time series data, and stores the properties of effect of parameter errors on the output. For example, while H (machine inertia) may shift the output response both horizontally and vertically, X_d (d-axis synchronous reactance) mostly effects the output response magnitude at the fault instant, during a disturbance. The mismatch provides various information on such properties of the power plant dynamic model when a parameter is biased. A training data is needed to characterize the parameter effect on the output response, similarly on the mismatch, to help the classification process. The idea is to teach the effect of parameter errors on the output response to the CNN model so that the erroneous parameters could be identified from the mismatch between the actual and simulated responses. In order to teach the model complete effect of a parameter on the output response, a detailed and balanced data generation process is necessary. The synthetic training data generation is summarized below.

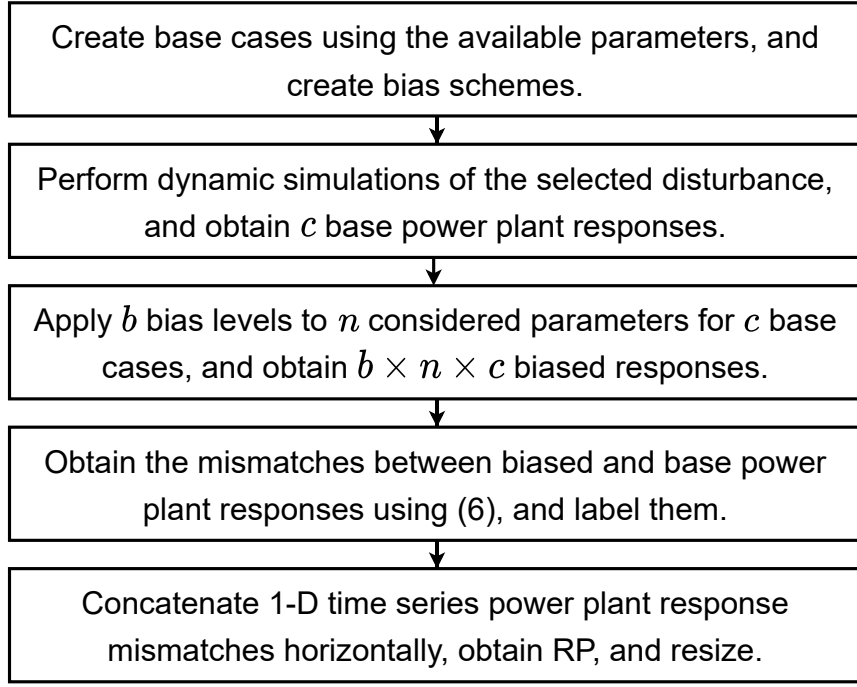


Figure 4.2: Flowchart of training data generation method.

First, available dynamic models of the network are reproduced with different scheduling and settings for the power plant. Each of these cases is called a base case. The disturbance is applied to each base case to obtain synthetically generated PMU data, which correspond to the base power plant responses to the selected disturbance. That is to say, the output response of the power plant during the selected disturbance event for each base case with different operation conditions are obtained, i.e. $P_{e,base}$ and $Q_{e,base}$, with the present dynamic parameters. Then, the sensitive parameters in the initial base cases are biased according to a bias scheme, and the biased output power plant responses, i.e. $P_{e,bias}$ and $Q_{e,bias}$, are obtained. Note that, the biased responses are obtained by biasing one parameter at a time.

The mismatches are calculated by subtracting the biased output responses from their corresponding base output responses, which is shown below. The training data set generation process is also summarized in Fig. 4.2.

$$\begin{aligned}
 P_{e,mismatch} &= P_{e,base} - P_{e,bias} \\
 Q_{e,mismatch} &= Q_{e,base} - Q_{e,bias}
 \end{aligned} \tag{4.1}$$

The power plant operating conditions and bias percentages must be selected accordingly to reveal their effects so that the CNN model is trained properly. For c base cases, n sensitive parameters, and b bias levels, the training set would contain $c \times n \times b$ mismatch pairs in (4.1). For a single mismatch, a bias is applied to a sensitive parameter in the given base case, and the biased response in that case is obtained. Then, it is subtracted from its bias-free version (base case).

The time series row vectors $P_{e,mismatch}$ and $Q_{e,mismatch}$ are concatenated horizontally to obtain a single time series data. Although this choice has advantages such as need of only a single classifier for each disturbance instead of two classifiers, and including the parameter error information of $P_{e,mismatch}$ and $Q_{e,mismatch}$ at once, different architectures could be used.

Each mismatch vector is labeled with the class that contains the biased parameter corresponding to the mismatch, by using one-hot encoding technique. At this point, a single sample data which has three classes in total, and has biased parameters in *Class 1* is shown as $[P_{mismatch} \ Q_{mismatch}] [1, 0, 0]$.

Although classification through 1-D time series signals is possible, 2-D classification may have higher performance in detecting the distinctive features compared to 1-D classification [17]. Therefore, 1-D time series mismatch vector is converted into 2-D images with the help of RP.

Dynamic events may last several seconds, and considering the resolution of PMUs, the time series data may be very large depending on the disturbance. The output of the RP transform is an $N \times N$ square matrix where N is the total data point, i.e. length of the time series data. The RP images could be downsized (ex. 64×64 or 128×128 pixels) depending on the disturbance duration, with any imaging library such as *PIL* in Python. Fig. 4.3 shows an example downsized RP, where N is 612 and the final RP is 128×128 . Note that, the gray points are result of the downsizing process. It is also worth to mention that, the reason for downsizing is to decrease the input size for memory considerations, it is not related to RP itself. Also, one must be aware of the trade off between accuracy and memory, i.e. accuracy decreases as the size decreases. At this stage, $c \times n \times b$ labeled and downsized recurrence plots corresponding to the mismatches are generated.

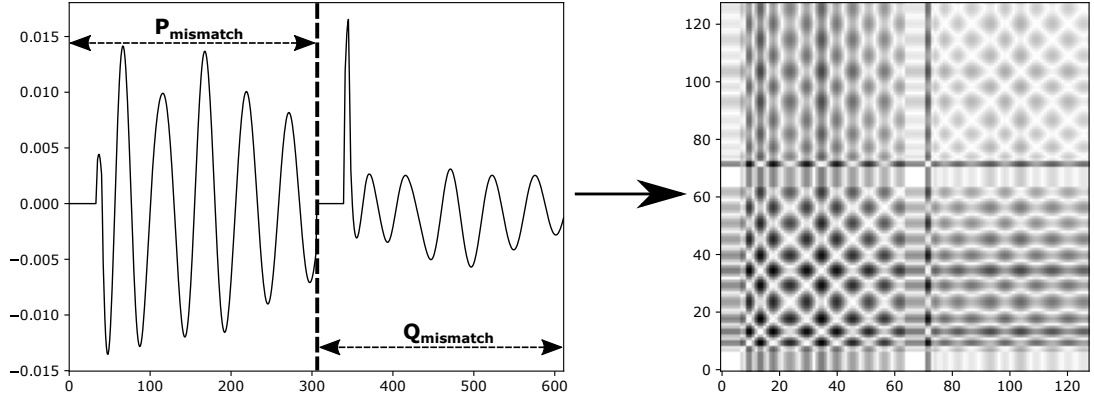


Figure 4.3: Time series power flow data to RP (downsized to 128×128 pixels).

4.4 CNN Architecture

CNN is one of the most used deep learning algorithms. Its main advantage is to extract features of the raw data without necessity for human supervision. It has a multi-layer structure which has an input layer, hidden layers and an output layer. The details about the implementation and layers of CNN can be found in [28]. In this thesis, a CNN architecture similar to [17] is adopted. The model has two convolutional layers with 32 feature maps, and 3×3 convolution. The convolutional layers are activated with *relu* function. At the end of each convolutional layer, a 2×2 MaxPooling layer is used for down-sampling, and a dropout layer with a rate of 0.2 is used to prevent over-fitting. Then, flattening, which is used to convert feature maps to 1-D vectors, is applied. Two fully connected layers are used. The first fully connected layer has 128 hidden layers, and it is activated with *relu*, and followed by a dropout layer with a rate of 0.5. For the last fully connected layer, *sigmoid* is used as activation function which is suitable for multi-label classification problems. As the optimizer and the loss function, "adam" and "binary cross entropy" are used, respectively.

4.5 Erroneous Parameter Identification

The proposed method identifies the erroneous power plant parameters one at a time, by a recursive algorithm composed of the trained CNN model and orthogonal decomposition. Once the model is trained for the selected disturbance event, the mismatch

between the power plant response and the collected PMU measurements is converted into RP as shown in Fig. 4.3, and fed into the model to start the identification process. The CNN model quantifies the possibility of existence of errors in each *Class* independently between 0 and 1, with the help of *sigmoid* activation function at the final layer. The *Class* corresponding to the highest and significant value is flagged as erroneous.

Once an erroneous parameter is identified, its effect is removed from the mismatch by using orthogonal decomposition in (2.8). In (2.8), u is the mismatch, v is the elementary effect of the *Class* that corresponds to the recently flagged erroneous parameter, and w^\perp is the residual mismatch. Thanks to the orthogonal projection, the effect of the identified erroneous parameter or *Class* is removed from the original mismatch. The next cycle starts with converting the residual mismatch into its RP, and continues with feeding its RP to the CNN and performing decomposition with respect to the identified erroneous parameter, until the termination condition is met. Note that, though the mismatches are fed into the CNN in their RP form, the decomposition is applied to time series data. The steps of the proposed error identification method is presented below.

Step 1: Convert the mismatch into its RP.

Step 2: Feed the RP of the mismatch into the classifier.

Step 3: Flag the parameter (or *Class*) that the classifier has the highest confidence of being erroneous. If a parameter (or *Class*) is flagged twice or confidence is low, terminate the process, else go to Step 4.

Step 4: Remove the individual effect of the flagged parameter (or *Class*) by using orthogonal decomposition in (5).

Step 5: If the residual mismatch is significant go to Step 1, else terminate.

Every flagged *Class* through the identification process correspond to a *Class* that contains erroneous parameters. After the projection, there may be some information loss in the residual mismatch due to non-zero dependency of the parameters. How-

ever, distinctive features of the mismatch will remain, which are the useful parts for the classifier.

Note that, a *Class* may contain one or more parameters depending on the collinearity analysis. Since the collinear parameters have similar effects on the power plant response, the residual mismatch may be projected onto either one of them. Grouping collinear parameters is very important step, since they are parameters are unidentifiable by their nature. However, the proposed method is able to localize the error on them as well. The algorithm of the proposed method is demonstrated in detail in Fig. 4.4.

4.6 Numerical Results

In this section, two case studies are presented in WSCC-9 Bus System. In this system, power plant of interest is chosen as the power plant connected to Bus 2, which consists of a GENROU model synchronous generator, an IEEE1 model exciter, an IEESGO model turbine governor, and a PSS2A model power system stabilizer. In total, the model has over fifty parameters including physical quantities as well as control parameters. Also, the model is slightly changed by setting the steady state active power injection and voltage magnitude values as $P_2 = 2p.u$ and $V_2 = 1.03p.u$ respectively. In this paper, eight sensitive parameters (H , X_d , X'_d , X''_d , K_E , T_7 , K_{S2} and K_{S3}) are used to present the results in a clear manner, although the method could be extended to higher dimensions without loss of generality. The equality $X''_d = X''_q$ holds throughout the results, however, only X''_d is shown for simplicity.

Test Case 1: A case study is created by applying a three phase symmetrical fault at the center of the transmission line between buses 4 and 6, then clearing it. The proposed method is applied to this selected disturbance. For another disturbance, the method must be applied from the start. In this test case, X'_d , K_E and T_7 were given 5% errors.

First, sensitivity analysis is carried out to determine the sensitive parameters for this disturbance. The sensitivity matrix S in (3.14) is constructed. By examining the norms of the columns, sensitive parameters are determined. Table 4.1 shows the total

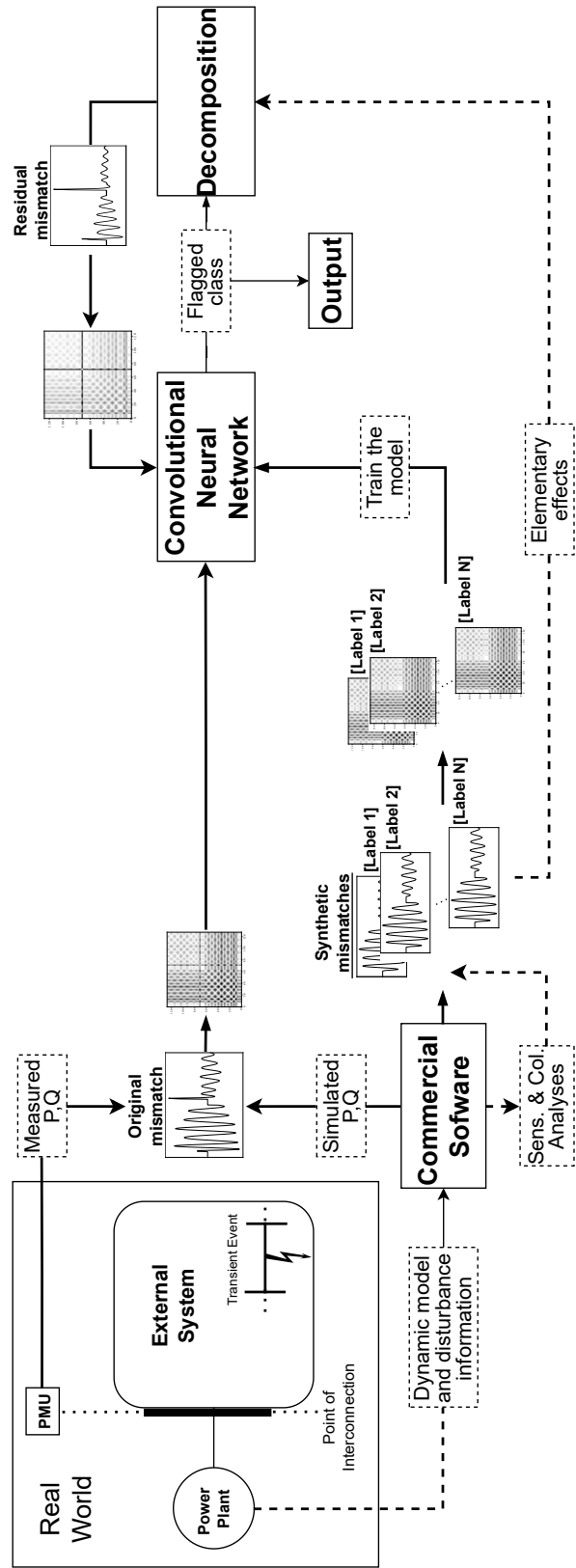


Figure 4.4: Flowchart of the proposed method.

sensitivities of the parameters, with respected to the applied disturbance.

Table 4.1: Parameter Sensitivities.

Parameter name	Total sensitivity
H – Inertia	0.625
X_d – d-axis synchronous reactance	0.255
X'_d – d-axis transient reactance	0.154
X''_d – d-axis subtransient reactance	0.170
K_E – Exciter constant	0.396
T_7 – PSS time constant	0.156
K_{S2} – PSS gain	0.157
K_{S3} – PSS gain	0.100

Then, the collinearity analysis is applied to the sensitive parameters in order to detect the collinearities and group the parameters into classes accordingly. The collinearity analysis results are shown in Fig. 4.5. Grouping of the parameters is done according to the collinearity analysis. Parameters with collinearity magnitude close to 1 are labeled as collinear parameters. Since the power plant response which corresponds to the perturbation on H is linearly independent from other disturbances, it is put into *Class 1*. However, X_d and K_E , and X'_d and X''_d , and T_7 , K_{S2} and K_{S3} create almost the same effects on the output response. Thus they are collinear parameters, and put into the same classes, *Class 2*, *Class 3*, and *Class 4* respectively. Labeling in synthetic data creation is done according to these classes.

The training data set is generated with the available parameters, where X'_d , K_E and T_7 were corrupted. While creating the training data, each parameter is applied perturbation of eight different bias levels within the interval $-4\% - 4\%$ for nine P and V settings. Then, the biased responses are subtracted from their base responses as shown in (4.1), and labeled with the corresponding *Class* labels. In order to obtain a balanced training data set, the mismatches created by error of each *Class* is generated equally. In total, 864 ($n = 12$, $c = 9$, and $b = 8$) labeled 1-D $[P, Q]$ mismatches are obtained, where approximately 20% is used for validation, and the CNN model is trained with the rest. Note that, every 1-D mismatch vector is converted to its corre-

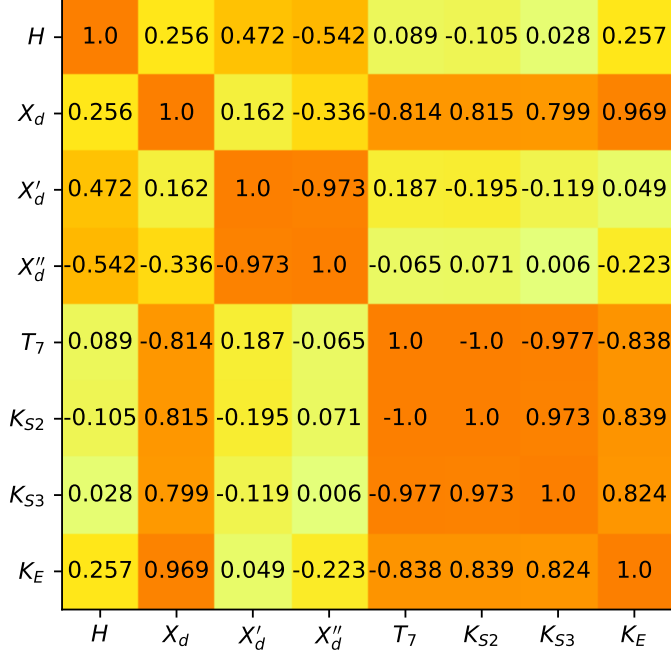


Figure 4.5: Collinearity Analysis Results.

sponding 128×128 pixels RP image as shown in Fig. 4.3 for training the 2-D CNN classifier.

The concatenated original corrupted 1-D mismatch is converted to its corresponding 128×128 pixels RP image, as well, and fed into the trained CNN to start the identification process. Prediction results for the test case is shown in Table 4.2, where the flagged classes are shown in bold. Initially, the error on *Class 2* is detected with high confidence. Hence, the orthogonal decomposition in (2.8) is used to eliminate the effect of the error on *Class 2* from the mismatch, where u is the mismatch, v is the elementary effect of *Class 2*, and w^\perp is the residual mismatch. The algorithm continues by advancing the process by using the residual mismatch, where the effect of the flagged erroneous classes are eliminated gradually. Fig. 4.6 shows the gradual elimination of the erroneous classes from the original mismatch. After the third iteration, the CNN could not flag any parameter with high confidence. Therefore, the identification process is terminated. Classes with erroneous parameters are identified successfully, and *Class 1* is removed from the potentially erroneous parameters subset.

Test Case 2: Another case study is created which is similar to the previous test case.

Table 4.2: Test 1 Results.

Iteration number	Class 1 H	Class 2 X_d, K_E^*	Class 3 X_d', X_d''	Class 4 T_7^*, K_{S2}, K_{S3}	Residual norm
Initial	1.07e-07	0.9946	5.00e-05	1.5e-13	2.382
1	3.38e-13	5.29e-15	1.0	1.00e-14	1.093
2	1.78e-04	4.71e-16	1.47e-13	0.9999	0.343
3	1.31e-05	2.58e-02	2.81e-04	5.47e-09	0.176

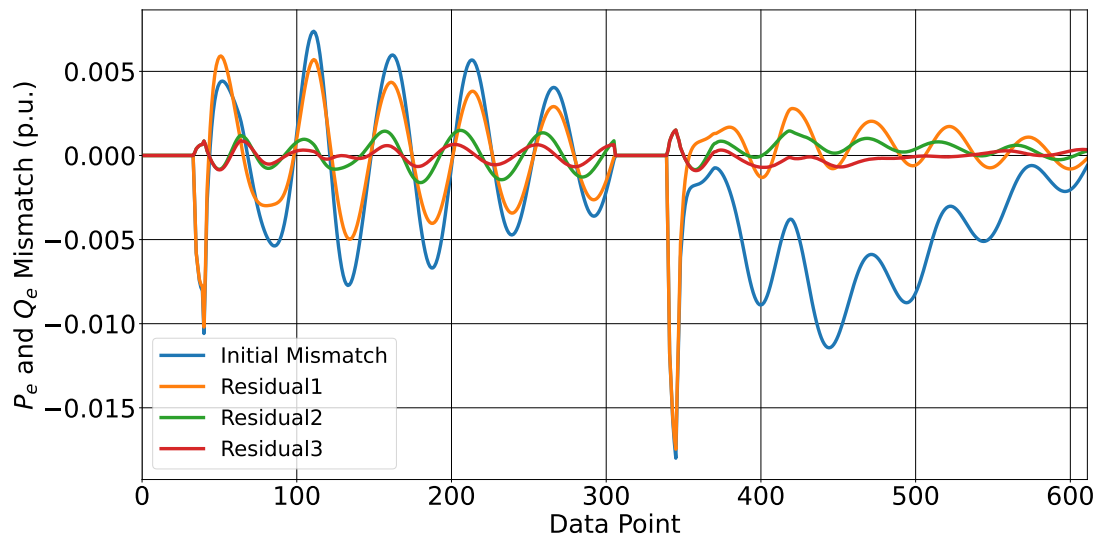


Figure 4.6: Test Case - 1 mismatch decomposition.

This time, H , X_d and K_{S3} are given errors. The identification process is restarted. The grouping is done as same as the previous case. The erroneous parameter identification results are shown in Table 4.3. Similarly, the classes which contain the erroneous parameters are identified step-by-step, as shown in Fig. 4.7. The residual of the third iteration is flagged as *Class 1* the second time. Hence, the identification process is terminated at the third iteration, since *Class 1* was already removed from the mismatch. Decomposing it with the same elementary effect would not affect the residual. At the end of the identification process, *Class 3* is found to contain only non-erroneous parameters. Also, the classes with erroneous parameters are identified. For further identification of erroneous parameters, another disturbance event data where the collinear groups differ must be utilized.

Table 4.3: Test 2 Results.

Iteration number	Class 1 H^*	Class 2 X_d^*, K_E	Class 3 X_d', X_d''	Class 4 T_7, K_{S2}, K_{S3}^*	Residual norm
Initial	0.9997	2.76e-03	6.06e-07	1.60e-08	4.468
1	3.00e-07	0.9978	1.41e-08	1.27e-02	1.799
2	0.3041	9.26e-09	6.41e-08	0.9617	0.723
3	0.9998	2.36e-05	1.58e-05	7.22e-06	0.510

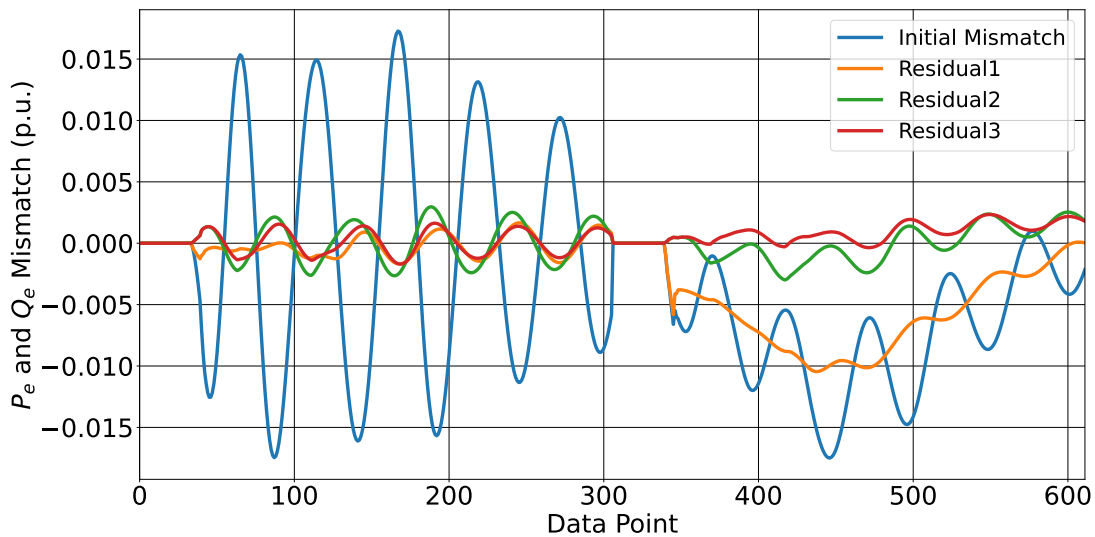


Figure 4.7: Test Case - 2 mismatch decomposition.

Note that, the proposed identification method is independent from the residual norm. Instead, the identification is done with respect to the signal waveforms. Therefore, the aim is not to achieve the minimum residual. However, a very small residual norm indicates the termination of the identification process as there may not remain any significant mismatch. This is due to approximate decomposition of the mismatch, and parameter dependence. In order to achieve minimum bias, the elementary effect of the flagged parameter or class must be selected carefully. The elementary effects which are used to train the CNN model could be utilized for this purpose.

The proposed method successfully identified the erroneous parameters (or classes), step-by-step. The traditional methods which aim to determine the identifiable parameters would mark all eight sensitive parameters as potential parameters to calibrate, and include all of them in the calibration process. Nevertheless, in Test Case 1 the parameter H in *Class 1*, and in Test Case 2 the parameters in *Class 3* do not contain errors. Including them in the calibration process may degrade the performance. The proposed method localized the parameter errors successfully. Thus, the flagged parameters (or classes) were removed from the candidate subset, which reduced the size of the problem. By this means, a smaller candidate parameter subset for calibration is achieved, and actual erroneous parameters (or classes) are identified.

4.7 Summary of the Chapter

Selection of candidate parameters is one of the key parts in power plant model calibration. Traditional methods in the literature utilize sensitivity analysis to determine identifiable parameters. These methods include the majority of the sensitive parameters to calibration process, and treat them as potentially inaccurate, without considering their possibility of being already calibrated. This thesis proposes a method to identify erroneous parameters. First, sensitivity and collinearity analyses are applied in order to determine sensitive parameters and collinearity groups, respectively. Then, a training dataset is synthetically generated by replicating the disturbance, and a CNN model is trained to identify the groups which contain erroneous parameters from the power plant response. By utilizing orthogonal decomposition, a recursive multiple parameter error identifier is realised.

The proposed method has a major advantage over classical multi-label classifiers, such that the proposed method does not need training data with every possible bias combination. The training data for the proposed method contain mismatches caused by only a single biased parameter at each time, which decreases the training data generation and model training times significantly.

The proposed method is tested on WSCC 9-Bus system, and successfully identified the actual erroneous parameters which reduced the size of the calibration problem significantly. The proposed method can be extended to multiple disturbance events, which may change the members of collinearity groups, hence the erroneous parameters within the classes can be further identified.

CHAPTER 5

CONCLUSION AND FUTURE WORK

Calibration of dynamic power plant models is of high importance in planning and control of power systems. It is a concern of system reliability, and one of the key elements for dynamic security assessment. Recently, the uncertainty in power systems increased due to the high penetration of renewable resources and change in the demand side. Therefore, the dynamic model reliability became an even more important concern for system operators. Traditionally, the dynamic power plant models are calibrated via offline staged tests. However, alternative methods are developed to replace them with remote calibration techniques based on PMU measurements, due to their high cost and high frequency. The remote calibration methods are developed with the motivation of continuous calibration of dynamic models, as the model parameters are prone to change due to physical effects and human errors. The remote dynamic model calibration consists of two main stages, the parameter selection and the calibration parts. This thesis presents two novel methods to enhance the parameter selection part, which also improves the calibration quality.

Most methods in the literature use sensitivity analyses to practically determine the identifiability of the dynamic model parameters based on a selected disturbance. They screen out the insensitive parameters, and provide a subset of sensitive parameters which are claimed to be identifiable. However, due to structural or numerical collinearity between the sensitive parameters, some of them may not be identifiable with existing data. Chapter 3 proposes a collinearity analysis method based on the *cosine* similarity and the trajectory sensitivity analysis, to detect the collinear parameters. By using different cases, it is shown that without additional data or information, the collinear parameters cause a threat to the calibration process.

The parameters that are sensitive and that do not have any collinear relation are identifiable. Nevertheless, this does not mean that all identifiable parameters must be included in the calibration process. The subset of identifiable parameters may contain error-free parameters. Inclusion of these parameters in the calibration process may decrease the accuracy. In Chapter 4, a novel parameter error identification method for power plant dynamic models is proposed. The method is based on the mismatch between the dynamic model response to a disturbance, and related PMU measurements. First, the disturbance is simulated on a commercial software and the effect of each parameter on the response is obtained as a 1-D time series data which is made of real and reactive power flows of the power plant model. Then, the simulated mismatch data are converted to RP, and a 2-D CNN model is trained. In this way, effect of each parameter is taught to the CNN model. A recursive algorithm is developed that identifies the erroneous parameters one by one. First, the CNN is fed with 2-D RP of the actual mismatch between the power plant dynamic model response and PMU measurements to the CNN, where the CNN flags the most possible erroneous parameter. The actual 1-D mismatch data are then projected onto the elementary effect of the flagged parameter, to remove its individual effect from the mismatch. Once the individual effect of the possible erroneous parameter is removed, the 2-D RP of the residual mismatch is fed to the CNN model again until one of the predetermined termination condition is met. As a result, the erroneous parameters of a power plant dynamic model is identified with an explainable approach, where the every step can be observed although it can be implemented in an autonomic manner. The method is validated on WSCC 9-bus test system with two test cases. The method is also enhanced with the proposed collinearity analysis method in Chapter 2, by grouping the collinear parameters.

This thesis concerns identifying erroneous parameters in a conventional power plant dynamic model. However, with the increased penetration of wind turbine generators to power systems, there have been increased research on dynamic models of the wind turbine generators. The erroneous parameter identification method that is developed in this thesis is a generic method that could be applicable to the dynamic models of wind turbine generators.

REFERENCES

- [1] J. Zhao, A. Gómez-Expósito, M. Netto, L. Mili, A. Abur, V. Terzija, I. Kamwa, B. Pal, A. K. Singh, J. Qi, Z. Huang, and A. P. S. Meliopoulos, “Power system dynamic state estimation: Motivations, definitions, methodologies, and future work,” *IEEE Transactions on Power Systems*, vol. 34, no. 4, pp. 3188–3198, 2019.
- [2] D. Kosterev, C. Taylor, and W. Mittelstadt, “Model validation for the august 10, 1996 wscs system outage,” *IEEE Transactions on Power Systems*, vol. 14, no. 3, pp. 967–979, 1999.
- [3] J. Zhao, M. Netto, Z. Huang, S. S. Yu, A. Gómez-Expósito, S. Wang, I. Kamwa, S. Akhlaghi, L. Mili, V. Terzija, A. P. S. Meliopoulos, B. Pal, A. K. Singh, A. Abur, T. Bi, and A. Rouhani, “Roles of dynamic state estimation in power system modeling, monitoring and operation,” *IEEE Transactions on Power Systems*, vol. 36, no. 3, pp. 2462–2472, 2021.
- [4] R. Huang, R. Diao, Y. Li, J. Sanchez-Gasca, Z. Huang, B. Thomas, P. Etingov, S. Kincic, S. Wang, R. Fan, G. Matthews, D. Kosterev, S. Yang, and J. Zhao, “Calibrating parameters of power system stability models using advanced ensemble kalman filter,” *IEEE Transactions on Power Systems*, vol. 33, no. 3, pp. 2895–2905, 2018.
- [5] A. Rouhani and A. Abur, “Constrained iterated unscented kalman filter for dynamic state and parameter estimation,” *IEEE Transactions on Power Systems*, vol. 33, no. 3, pp. 2404–2414, 2018.
- [6] M. González-Cagigal, J. Rosendo-Macías, and A. Gómez-Expósito, “Parameter estimation of fully regulated synchronous generators using unscented kalman filters,” *Electric Power Systems Research*, vol. 168, pp. 210–217, 2019.
- [7] Z. Huang, P. Du, D. Kosterev, and S. Yang, “Generator dynamic model validation and parameter calibration using phasor measurements at the point of con-

- nection,” *IEEE Transactions on Power Systems*, vol. 28, no. 2, pp. 1939–1949, 2013.
- [8] S. Wang, R. Diao, C. Xu, D. Shi, and Z. Wang, “On multi-event co-calibration of dynamic model parameters using soft actor-critic,” *IEEE Transactions on Power Systems*, vol. 36, no. 1, pp. 521–524, 2021.
- [9] E. L. Geraldi Jr, T. C. Fernandes, A. B. Piardi, A. P. Grilo, and R. A. Ramos, “Parameter estimation of a synchronous generator model under unbalanced operating conditions,” *Electric Power Systems Research*, vol. 187, p. 106487, 2020.
- [10] S. R. Khazeynasab and J. Qi, “Generator parameter calibration by adaptive approximate bayesian computation with sequential monte carlo sampler,” *IEEE Transactions on Smart Grid*, vol. 12, no. 5, pp. 4327–4338, 2021.
- [11] S. R. Khazeynasab, J. Zhao, I. Batarseh, and B. Tan, “Power plant model parameter calibration using conditional variational autoencoder,” *IEEE Transactions on Power Systems*, pp. 1–1, 2021.
- [12] Y. Xu, L. Mili, X. Chen, M. Korkali, and L. Min, “A bayesian approach to real-time dynamic parameter estimation using phasor measurement unit measurement,” *IEEE Transactions on Power Systems*, vol. 35, no. 2, pp. 1109–1119, 2020.
- [13] Y. Xu, L. Mili, M. Korkali, and X. Chen, “An adaptive bayesian parameter estimation of a synchronous generator under gross errors,” *IEEE Transactions on Industrial Informatics*, vol. 16, no. 8, pp. 5088–5098, 2020.
- [14] Y. Xu, C. Huang, X. Chen, L. Mili, C. H. Tong, M. Korkali, and L. Min, “Response-surface-based bayesian inference for power system dynamic parameter estimation,” *IEEE Transactions on Smart Grid*, vol. 10, no. 6, pp. 5899–5909, 2019.
- [15] U. Agrawal, P. Etingov, and R. Huang, “Advanced performance metrics and their application to the sensitivity analysis for model validation and calibration,” *IEEE Transactions on Power Systems*, vol. 36, no. 5, pp. 4503–4512, 2021.
- [16] P. Wang, Z. Zhang, Q. Huang, W. Zhang, and W.-J. Lee, “Pmu based problematic parameter identification approach for calibrating generating unit models,”

- IEEE Transactions on Industry Applications*, vol. 57, no. 5, pp. 4520–4527, 2021.
- [17] N. Hatami, Y. Gavet, and J. Debayle, “Classification of time-series images using deep convolutional neural networks,” in *Tenth international conference on machine vision (ICMV 2017)*, vol. 10696, p. 106960Y, International Society for Optics and Photonics, 2018.
- [18] N. Marwan, M. Carmen Romano, M. Thiel, and J. Kurths, “Recurrence plots for the analysis of complex systems,” *Physics Reports*, vol. 438, no. 5, pp. 237–329, 2007.
- [19] R. Brun, P. Reichert, and H. R. Künsch, “Practical identifiability analysis of large environmental simulation models,” *Water Resources Research*, vol. 37, no. 4, pp. 1015–1030, 2001.
- [20] I. A. Hiskens, “Nonlinear dynamic model evaluation from disturbance measurements,” *IEEE Transactions on Power Systems*, vol. 16, no. 4, pp. 702–710, 2001.
- [21] S. M. Benchluch and J. H. Chow, “A trajectory sensitivity method for the identification of nonlinear excitation system models,” *IEEE Transactions on Energy Conversion*, vol. 8, no. 2, pp. 159–164, 1993.
- [22] K. Z. Yao, B. M. Shaw, B. Kou, K. B. McAuley, and D. Bacon, “Modeling ethylene/butene copolymerization with multi-site catalysts: parameter estimability and experimental design,” *Polymer Reaction Engineering*, vol. 11, no. 3, pp. 563–588, 2003.
- [23] P. W. Sauer, M. A. Pai, and J. H. Chow, *Power system dynamics and stability: with synchrophasor measurement and power system toolbox*. John Wiley & Sons, 2017.
- [24] Y. Xu, L. Mili, X. Chen, M. Korkali, and L. Min, “A bayesian approach to real-time dynamic parameter estimation using phasor measurement unit measurement,” *IEEE Transactions on Power Systems*, vol. 35, no. 2, pp. 1109–1119, 2019.

- [25] J. Zhao, M. Netto, and L. Mili, "A robust iterated extended kalman filter for power system dynamic state estimation," *IEEE Transactions on Power Systems*, vol. 32, no. 4, pp. 3205–3216, 2016.
- [26] J. Han, J. Pei, and M. Kamber, *Data mining: concepts and techniques*. Elsevier, 2011.
- [27] A. R. Al-Roomi, "Power Flow Test Systems Repository," 2015.
- [28] A. Dhillon and G. K. Verma, "Convolutional neural network: a review of models, methodologies and applications to object detection," *Progress in Artificial Intelligence*, vol. 9, no. 2, pp. 85–112, 2020.